

IMPACT OF ENERGY MANAGEMENT IN A SOLAR PV MICROGRID

Elias Onyango Apiyo

**A Thesis Submitted in Partial Fulfillment of the Requirements for the Degree of
Master of Technology in Electrical and Electronic Engineering of Murang'a
University of Technology**

November, 2022

DECLARATION

I hereby, declare that this thesis is my original work and to the best of my knowledge has not been presented for a degree award in this or any other university.

Elias Onyango Apiyo

EN400/5078/2018

Date

APPROVAL

The undersigned certify that they have read and hereby recommend for acceptance of Murang'a University of Technology a thesis entitled "**Impact of Energy Management in a Solar PV Microgrid**".

Prof. Eng. Christopher Maina Muriithi

Department of Electrical and Electronics Engineering

Murang'a University of Technology

Date

Prof. Eng. Livingstone Mwalugha Ngoo

Department of Electrical and Telecommunications Engineering

Multimedia University of Technology

Date

ACKNOWLEDGEMENT

Primarily, I praise God the Almighty for giving me His blessings during my study.

The research conducted in this thesis resulted from a collective work as contributions from various parties supporting the thesis were involved.

My sincere thanks go to my supervisors Eng. Prof. Christopher M. Muriithi and Prof. Eng. Livingstone M. Ngoo for their tireless, kindness, generous support and strong encouragement right from the conceptual framework of this thesis. Thank you all and God bless you.

I gratefully thank Job Masika Wekesa of Murang'a University of Technology for the humble contribution in microcontroller programming support offered towards the development of this thesis. The support was helpful in hardware implementation and thesis writing process. God bless you.

Lastly, my sincere thanks goes to Yusuf Abdiwali Mohamed of the Technical University of Kenya for the humble contribution in software development programs related to weather forecasting that proved useful to this thesis. Praise Allah the Almighty.

ABSTRACT

Fossil fuel accounts for a bigger percentage of primary energy sources in the world. Studies show that the world energy demand is on the rise but the real sources of fossil fuel decline each day. Major oil producing countries are likely to deplete their oil fields within a decade if the current rate of fossil fuel production maintained. Generation of energy through fossil fuel burning causes Greenhouse Gas Emission into the atmosphere causing global warming. Generation of energy through renewable energy sources provides a better alternative to cope with the declining oil reserves and combat climate change. Solar photovoltaic is a suitable alternative clean and environmentally friendly renewable energy source, which uses solar photovoltaic technology. This thesis discussed the impact of energy management on a solar photovoltaic microgrid and tried to narrow the research gap left by various researchers who provided related literature about the work. Modeling, energy management and the impact of installing solar PV system to supplement utility grid electricity is studied. This work was conducted using a mathematical model of the PV based microgrid that was simulated using MATLAB/Simulink software. The laboratory implementation was done using hardware components and real-time energy management using microcontroller. The prediction of solar PV power generation on a medium-term basis was done using PVsyst photovoltaic software while a short-term basis was implemented using Application Programming Interface software. The energy management strategy is such that the solar PV module becomes the priority power source to supply three loads while charging the battery when irradiance is sufficient. At low irradiance, the battery supplies the loads and when the discharge is below a specified limit, the utility grid electricity supplies the loads. Simulation results show that the solar PV module serve the loads and charge the battery during daytime while the grid remained as a standby power source. However, the microcontroller disables the loads from the PV system source when the threshold of charging the battery is reached. The loads are then connected to the utility grid. In the simulation of the solar resource software, the solar pv generation for seven days on the month of March 2022 indicated a maximum and minimum generation of 720.82 Wh and 498.96 Wh respectively. The financial analysis of installing 90 W grid-tied PV solar system without subsidy is US\$ 384. The 90 W module costs US\$ 486 and has a service life of 25 years and payback period of 11 years. During the lifespan of the solar PV module, 1,333.78 kg of CO₂ emitted into the atmosphere are saved.

TABLE OF CONTENTS

DECLARATION	ii
ACKNOWLEDGEMENT	iii
ABSTRACT	iv
LIST OF TABLES	ix
LIST OF FIGURES	x
ACRONYMS AND ABBREVIATIONS	xi
CHAPTER ONE: INTRODUCTION	1
1.1 Background of the Study.....	1
1.2 Statement of the Problem.....	4
1.3 Study Objectives.....	5
1.3.1 General Objective.....	5
1.3.2 Specific Objectives.....	5
1.4 Research Questions.....	6
1.5 Significance of the Study.....	6
1.6 Scope of the Study.....	7
1.7 Delimitations and Limitations.....	8
1.8 Conceptual Framework.....	8
1.9 Contributions of the Thesis.....	9
1.10 Thesis Organization.....	10
CHAPTER TWO: LITERATURE REVIEW	11
2.1 Introduction.....	11
2.2 Solar Photovoltaic Arrays.....	11

2.2.1	Photovoltaic Technology	11
2.2.2	Monocrystalline Solar Panels	13
2.2.3	Polycrystalline Solar Panels.....	14
2.2.4	Photovoltaic Cell Voltage	14
2.2.5	Derating in PV Array	15
2.2.6	Components of a Solar PV System	16
2.2.7	Location Issues.....	17
2.3	Energy Storage System	18
2.3.1	Battery Types	19
2.3.2	Battery Management	23
2.4	Microcontrollers	24
2.4.1	Microcontroller Architecture	25
2.4.2	Desirable Features of a Microcontroller	27
2.4.3	Arduino Microcontroller	27
2.5	Impact of Solar PV System Installation	30
2.5.1	Environmental Impact.....	31
2.5.2	Financial Impact.....	32
2.5.3	Social Impact	33
2.6	Related Literature on Solar Photo-Microgrids	33
2.7	Current Trends in Microgrid Energy Management.....	39
2.8	Summary	43
	CHAPTER THREE: METHODOLOGY.....	44
3.1	Introduction	44

3.1.1	Selection of Simulation Software	44
3.1.2	Site Location	47
3.1.3	Data Collection	48
3.2	Microgrid Modeling	49
3.2.1	Mathematical Modeling of Microgrid Components	49
3.2.2	Solar PV System Sizing	56
3.3	Real-time Energy Management of the Microgrid	61
3.3.1	Hardware Implementation.....	62
3.3.2	Software Algorithm	64
3.4	Estimation of Future Solar Power Production.....	66
3.4.1	Medium-term Weather Forecast	67
3.4.2	Short-term Weather Forecast	68
3.5	Validation of the Proposed EMS.....	69
3.5.1	Cost Analysis	69
3.5.2	Payback Period.....	71
3.5.3	Net Present Value	72
3.6	Summary	72
CHAPTER FOUR: RESULTS AND DISCUSSION		73
4.1	Introduction	73
4.2	Results of Modeling and Simulation.....	73
4.3	Real-time Energy Management.....	75
4.4	Weather Forecasting.....	75
4.5	Economic Benefits	79

4.6	Environmental Impact	80
4.7	Social Impact	81
CHAPTER FIVE: CONCLUSION AND FUTURE WORK.....		82
5.1	Conclusion.....	82
5.2	Future Work of the Study	83
REFERENCES.....		84
APPENDICES		93

LIST OF TABLES

Table 3.1 Load Consumption.....	57
Table 3.2: Characteristics of Yingli solar PV module	58
Table 3.3: Component and other costs estimate	71
Table 4.1 Monthly Global irradiance (Nairobi).....	76
Table 4.2: Summary of GHI and temperature, (Murang'a), March 12 th through 17 th	78

LIST OF FIGURES

Figure 2.1: Construction of a solar cell.....	12
Figure 2.2: Effect of inclination on a PV module.....	17
Figure 2.3: Lead-acid battery discharge mode.....	21
Figure 2.4: Microcontroller architecture.....	25
Figure 2.5: Arduino Uno board.....	30
Figure 3.1: Single diode model of a solar cell.....	50
Figure 3.2: Simulink model of a solar PV module.....	52
Figure 3.3: Simulink model of a generic lead-acid battery.....	53
Figure 3.4: Simulink model of a bridge inverter.....	54
Figure 3.5: Complete microgrid subsystems.....	56
Figure 3.6: Proposed microgrid energy management system.....	62
Figure 3.7: Microgrid experimental set up.....	64
Figure 3.8: Energy management flow chart algorithm.....	66
Figure 4.1: Simulated results of power_load, power_PV, power_grid, and battery SOC.....	74
Figure 4.2: Forecast Global irradiance (Murang'a), March 11 th through 17 th	78

ACRONYMS AND ABBREVIATIONS

API	Application Programming Interface
BESS	Battery Energy Storage System
DoD	battery Depth of Discharge
EMS	Energy Management System
EPA	United States Environmental Protection Agency
EPRA	the Energy and Petroleum Regulatory Authority
GHG	Greenhouse Gas
GHI	Global Horizontal Irradiance
IDE	Integrated Development Environment
IRENA	International Renewable Energy Agency
NPV	Net Present Value
OPEC	The Organization of Petroleum Exporting Countries
PV	Solar Photovoltaic
SOC	Battery State of Charge
SOH	State of Health
VRLA	Voltage Regulated Lead-acid Battery

CHAPTER ONE

INTRODUCTION

1.1 Background of the Study

Electricity is an essential service in modern life and world economy. People use electricity for operating appliances, heating, cooling, lighting, machinery and public transport. Fossil fuel burning accounts for a bigger percentage of current sources of world electricity with the demand for electricity increasing each day. The production of electricity from fossil fuel combustion leads to increase in Greenhouse gas (GHG) emission into the environment and destruction of ozone layer. The United States climate agency estimates the CO₂ levels in the atmosphere at 50% higher than pre industrial era. Countries were requested, through climate change conferences, to bring forward the ambitious 2030 emissions reduction targets that align with reaching net zero by the middle of the century [1]. To achieve this, countries will need to phase out fossil fuel burning and encourage investment in renewables. Solar power is one of the promising renewable energy source currently on the rise.

The PVsyst photovoltaic software estimates the Kenya's solar potential measured in irradiance at 5.11 kWh/m²/day making the country potentially favorable for photovoltaic power generation.

Solar panels depend on solar radiation to produce its power. The maximum power is obtained on a clear sunny weather (higher insolation) while the power ranges between 10% to 30% on a cloudy day.

Solar energy is intermittent because the sun's intensity is not always constant but varies at different times of the day depending on location. The sun only shines for some hours not all hours in a day. The intermittent nature of solar energy makes it impossible for consistent use without an electricity storage system that overcomes the intermittency. The electricity storage is a research field that has attracted many researchers. To maintain constant load supply, the surplus electricity needs to be stored during sunny hours of the day and the stored electricity used when the solar radiation drops. Battery energy storage systems (BESS) are widely used for electricity storage in solar photovoltaic (PV) systems.

Research conducted in [2] concluded that the solar cell output power is affected by shadow, dust, snow, and rain, but rainwater saves some of the maintenance efforts by washing away the dirt, affecting its output positively. For better understanding of the solar physical system, mathematical models of the solar PV components are simulated using MATLAB/Simulink software. The solar PV system components are sized based on the least weather data collected at the study site. Real-time implementation using a prototype for the proposed system is carried out, and the energy management between the load and the microgrid sources is achieved by incorporating an Arduino microcontroller and sensors. Smart energy management is necessary for efficient production and consumption of solar power, maintaining the health status of PV system components, reducing the dependency on utility grid electricity, thereby reducing electricity bills and also reducing the GHG emissions into the atmosphere.

Accurate weather forecast software can serve as a weather station set to forecast weather parameters (irradiance and temperature) around the study site. With the prior

knowledge of weather data around the study site, it is possible to predict future power generation pattern from the solar PV module. Such predictions are useful for short term and medium term planning generally called economic dispatch.

Application Programming Interface (API) software provides accurate weather parameters like irradiance, air temperature and cloud opacity. The air temperature and irradiance data are the main input parameters used in simulating the PV system to estimate the actual future PV power generation. The API allows communication with Google services for easy download of live and forecast solar radiation data [3]. The application software is suitable for up to 7-day weather forecast in the study site. Feasibility study is usually conducted before venturing into an investment and the financial indicators like payback period and net present value evaluated to assess the feasibility of the project based on the resource potential of the study site. In addition, assessment of environmental and social impact of a project is necessary prior to its development. In this work, both the positive and the negative impacts arising from the installation of the solar PV system to supplement the utility grid electricity are evaluated.

The work assessed the impact of energy management in a 90 W grid tied solar PV system with real implementation using hardware components in the laboratory at Murang'a University of Technology. The study predicted the future PV power generation of the installed capacity using software programs and data from the weather station.

The subsequent sections presented the statement of the problem, the study objectives, significance of the study, the scope of the study and the list of publications from the thesis.

1.2 Statement of the Problem

World economies have been heavily reliant on nonrenewable fossil fuels such as oil, coal and natural gas as the primary source of power for decades. Currently, fossil fuels account for about 80% of the world's known primary sources of energy [4]. The energy consumption rate in the world is ever increasing each day but the available resources remain limited and hence pose the risk of depleting the available resources in the near future. Generation of energy through burning of fossil fuel causes greenhouse gas emission into the atmosphere leading to global warming and destruction of ozone layer.

The rising oil prices, depletion of fossil fuel and the need to combat climate change has led to development of alternative technologies of producing electricity from renewable energy sources, that are cleaner while assisting to combat climate change. Solar photovoltaic technology, which capture and directly convert sunlight into electrical energy, is taking the lead as an alternative to energy generation instead of fossil fuel burning. Combining the solar PV power with the utility grid electricity has been a challenge to many solar PV installations currently in place leading to their short lifespan. Photovoltaic generation does not have the luxury to generate power on demand because its power generation depends on the prevailing weather condition of the day and thus require storing excess energy for later use. Poor energy management may lead to underutilization of the solar PV power generated or overutilization of the

storage device used leading to short life of the solar PV system. If properly applied, EMS is able to reduce the cost of grid electricity by reducing the wastage in power usage. Shifting electricity demand by encouraging customers to use electricity when it is more readily available is not possible without proper EMS. Some solar PV projects fail to pick up because of poor feasibility studies as no proper financial analysis done before investing in such projects. This indicates that there is still some research gaps that need narrowing to improve the situation while calling for efficient energy management between the solar PV system and the utility grid electricity. It is the aim of this study, as in the literature, to fill the gap and improve the stability of the solar PV installations.

1.3 Study Objectives

1.3.1 General Objective

The main objective of the study is to determine the impact of energy management in a solar Photovoltaic microgrid.

1.3.2 Specific Objectives

The researcher's specific objectives shall be:

- i. To model a PV based microgrid system to reduce the fossil fuel contribution to utility grid electricity.
- ii. To perform real-time energy management of the modeled microgrid.
- iii. To estimate future solar power production on medium and short term basis.
- iv. To validate the energy management system of the proposed microgrid.

1.4 Research Questions

The research questions that arise in pursuit of the above objectives are as follows:

- i. What are the economic, social and environmental impacts of installing a solar PV system to supplement utility grid electricity?
- ii. What changes must be made to existing models to more accurately reflect the value of microgrids? Can the user monitor solar PV parameters in real-time?
- iii. Can the user predict solar PV production for next day?
- iv. By integrating renewable energy to the utility grid, what percentage can be reduced on utility grid electricity per day?

1.5 Significance of the Study

The world has heavily relied on fossil fuels as its primary energy source to sustain its fast growing energy demand. The continued dependency on fossil fuel to cope with the rapid economic growth will eventually exacerbate the GHG emission into the atmosphere and climate change. The rising cost of fuel by the Organization of the Petroleum Exporting Countries (OPEC) has negative impact on both the cost of living and the cost of generation and consumption of electricity. Reducing the dependency on fossil fuel by using renewable energy resources is necessary to overcome these disadvantages. Solar energy as a renewable energy source has lower initial cost as compared to the fossil fuel option. Research conducted by the International Renewable Energy Agency (IRENA) 2020 shows that 62% of the total generation added from renewable resources had lower fast costs than fossil fuel option [5]. Solar photovoltaic system is one of the world's promising renewable energy sources having many

advantages compared to nonrenewable sources. Solar energy (insolation) is freely available, environmental pollution resulting from its use is minimal, its operation is quiet with no noise nor exhaust, production end wastes manageable by applying engineering controls. The maintenance of PV systems requires minimum maintenance during the operation period because there are no moving parts which are liable to breakdown. The warranty period of a solar panel is many years in healthy state with little linear annual output degradation rate. PV system can easily be installed and operated in remote locations while at the same time can be easily expanded to larger sizes. Installing on-grid solar PV system reduces the utility grid electricity cost. Mathematical modeling equations that can be easily formulated and simulated are used to represent the real-time performance of a solar PV system. Affordable microcontrollers are readily available that can be incorporated with other hardware components to demonstrate the proposed EMS. Available solar resource software are readily available in the internet upon registration or subscription to aid in the forecast of future PV power generation.

1.6 Scope of the Study

This study assesses the impact of energy management in a solar PV microgrid with emphasis on Murang'a University of Technology. The university was purposely selected because it is a research Centre with potential researchers and plenty of solar radiation. The study is limited to mathematical modeling of the PV based microgrid, energy management of the microgrid, financial analysis and the environmental impact resulting from the proposed energy management system. The model uses MATLAB/Simulink software in modeling the microgrid components, which include

solar PV module, BESS, power inverter and utility grid electricity. The same microgrid components are sized according to the standard photovoltaic power installation requirements. The study conducted real-time implementation of the energy management system in the laboratory using hardware components. The proposed system also predicts medium term and short-term PV power production based on on-line weather forecast software. The study further assesses the feasibility of installing the solar PV system to supplement the utility grid electricity and quantifies the amount of GHG emission reducible by switching from the utility grid to solar PV system for the entire life of the project.

1.7 Delimitations and Limitations

This study explored the impact of energy management in a solar PV microgrid at Murang'a University of Technology. The site selected because of its readily available utility grid connection point and has sufficient sunlight at rooftops for solar power production. The limitations of the study were mostly experienced at design stage since most of the required simulation software sourced was a trial version that lasted for a few days to a month after which sourcing the particular software becomes difficult, this stalled the pace of the study.

1.8 Conceptual Framework

High electricity prices, depletion of fossil fuel resources and need to combat climate change has led to generation of electrical energy through renewable energy sources with solar PV system taking the lead. In this study, the proposed load management system modeled and implemented consists of a single-phase 55 W load supplied from two sources of energy i.e. the solar PV system power and the utility grid electricity.

The solar PV system consists of a roof top solar module and a battery storage system. The solar PV module generates its electric power through solar photovoltaic technology from the sun during the day and charges the battery. During the night or on a poor weather, the battery assumes the responsibility of the PV module and supplies the load. The solar PV system supplies the load through DC-AC power inverter whereas the single-phase 240 V power supply obtained from the utility grid supplies the load directly. To achieve the energy balance between the two sources of power supply, Arduino Uno microcontroller, sensors and relays are used to switch the connected load between the two sources of power. Additional software was used to enable prediction of future power production from the solar PV module. The software collects weather parameter of irradiance and temperature of the study site used as input parameters for the model simulation. The financial analysis of the proposed load management to validate the feasibility of installing the PV based microgrid and the potential CO₂ offset or environmental impact arising from such installations studied.

1.9 Contributions of the Thesis

The contributions made by this study are highlighted below:

- i. MATLAB/Simulink software was used in modeling the solar PV system and simulated to represent the real time performance of the PV system.
- ii. A prototype was developed to demonstrate the proposed energy management system within the modeled PV system.
- iii. A new method of weather forecasting software was used for quantitative prediction of future solar PV power generation on a medium and short-term basis.

- iv. Economic, environmental and social impact of solar PV system venture was studied and the investment proved viable.
- v. Journal papers containing the results of this study have been published.

1.10 Thesis Organization

The overview of the remaining sections of the thesis layout provided. Chapter 2 discusses the literature review on solar photo microgrids covering the current trends in photovoltaic system technology and related studies conducted by other researcher in the solar photovoltaic sector. Chapter 3 gives the methodology used to achieve the set objectives; solar PV modeling, real-time energy management using a microcontroller, financial validation of the proposed energy management system and various weather forecasting methods. Chapter 4 presents the results and discussion based on the study findings and guided by the study objectives. Chapter 5 is the conclusion of the work and prospects of future work.

CHAPTER TWO

LITERATURE REVIEW

2.1 Introduction

In this section, the literature review on solar PV system is discussed with emphasis on the theory behind the solar PV technology, the energy storage technologies used, the smart energy management system and its overall impact. The section also focuses on related literature review from various researchers conducted on solar PV microgrids. The chapter collects relevant information from the past literature in order to narrow the research gap left by the past researchers. The current trends in energy management are also discussed and gaps identified.

2.2 Solar Photovoltaic Arrays

The sun's energy is freely available and will not end soon hence inexhaustible in nature. The solar power is renewable and environmentally friendly while not any GHG emission to the environment. Silicon, which is the primary component in solar cell manufacturing, is the second abundantly available element in the earth's crust. Solar power in photovoltaic form has proved efficient both in residential and commercial use. Government incentives has led to price cuts in the cost of solar PV system and hence making it affordable.

2.2.1 Photovoltaic Technology

A Solar cell also called solar photovoltaic cell converts sunlight into electricity by the principle of photovoltaic effect. Alexandre-Edmond Becquerel, French physicist

(1839) discovered the photovoltaic effect in an electrolytic cell with two platinum electrodes. Real implementation of the solar cell started in 1954 in the United States Bell Laboratories by the scientists Daryl M. Chapin, Calvin S. Fuller, and Gerald L. Pearson using silicon solar cell [6]. All solar cells are mainly made up of silicon semiconductor material having different doping levels. The n -type layer and the p -type layer and a thin film layer between the p -type and the n -type layers (also called metallurgical junction) behaves like a capacitor stretching electric field formed by the two layers across it. A large difference in electron concentration in the n -type layer and holes in the p -type layer. This causes the flow of electrons from the n -type region across the metallurgical junction to the p -type layer. This flow of electrons from the n -type region to the p -type region constitute electric current, which flows to the external circuit when an external load circuit is connected. Figure 2.1 shows the construction of a silicon semiconductor solar cell.

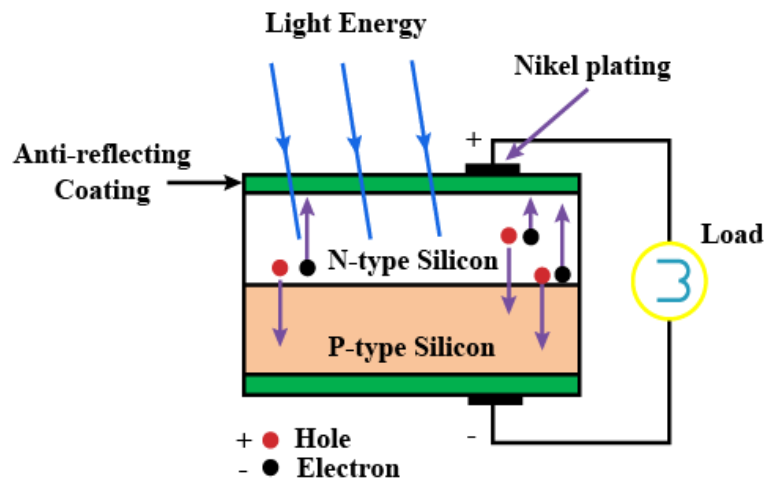


Figure 2.1: Construction of a solar cell [7]

The three main technologies used in PV cell manufacturing are monocrystalline silicon, polycrystalline silicon and thin film [8]. The similarities and differences in the

technologies are broken down with regard to cost and efficiency for better choice of solar installation.

2.2.2 Monocrystalline Solar Panels

A single pure silicon crystal makes the solar PV cell of this category. Monocrystalline solar panels are the oldest and most developed. They are characterized by their rounded edges and black PV cells. The lifespan and the efficiency level of the solar panel has been the main problem in the market today. The solar PV module efficiency can be formulated as the ratio of its output power to input power expressed as a percentage (2.1).

$$\eta = \frac{P_{out}}{P_{in}} \times 100\% \quad (2.1)$$

Where η denotes the efficiency of the solar PV module, P_{in} and P_{out} are the power input and output of the PV module in watts respectively.

The comparative analysis conducted in [9] to determine the effectiveness of a 50 W monocrystalline silicon PV panel and a polycrystalline PV panel of the same rating concluded that a monocrystalline solar panel is 14.51% efficient whereas a polycrystalline PV panel is 13.75% efficient. Monocrystalline solar panel is able to convert more solar radiation into electricity than the polycrystalline panel of the same power rating under same operating conditions. In areas with limited space, economics of scale discrete the installation of this type of panel as opposed to the polycrystalline panels. The manufacturing process of monocrystalline solar panels is more complex and expensive as compared to the polycrystalline silicon type of the same capacity.

2.2.3 Polycrystalline Solar Panels

Polycrystalline solar panels are a newer version in photovoltaic development and are quickly picking up. Multiple fragments of silicon crystal are melted together in the manufacturing of polycrystalline solar cells. Their manufacturing process is simpler than the monocrystalline type and this makes them cheaper. Solar panels of this type are blue-hued in color with straight edges. Their efficiency as calculated using equation (2.1) is lower than a monocrystalline type of the same rating, and hence more panels are required to deliver the same power output. Polycrystalline solar panels are affected by high temperature and hence their output during hotter days is reduced while their lifespan also slightly lower than the monocrystalline solar panels of same capacity.

2.2.4 Photovoltaic Cell Voltage

Irradiance and temperature are the two main input parameters of a solar cell that determine the output voltage and current. The amount of voltage produced by one silicon solar cell is small. The open circuit voltage of a polycrystalline solar cell is typically about 0.57 V at 25°C. When connected to a load, the terminal voltage drops to about 0.46 V at 25°C. In order to form a solar module, a number of such cells are connected in series and the connection of several such modules form a solar array. A solar panel can be made up of 32, 36, 60, 72 or 96 solar cells with a 32 solar cell panel producing 14.72 V. When the temperature of a PV module is increased, the output voltage decreases considerably but the output current is slightly increased. At higher temperatures, both the semiconductor bandgap and internal energy losses increase

leading to a decrease in open circuit voltage and slightly increased short circuit current. At higher temperatures, PV modules are highly stressed and hence their lifetime is reduced. With a decrease in irradiance, the output voltage slightly decreases and the output current decreases proportionally [10] . The output power of a solar module decreases with temperatures above 25°C and increases with temperatures below 25°C.

2.2.5 Derating in PV Array

Local vegetation, building infrastructure, landform or foreign materials on the surface of a PV array may greatly affect its output if this occurs during the active sunshine hours. Shading reduces the amount of solar irradiation reaching the PV array. The least level of solar irradiation should be the reference in determining the required size of PV array needed to provide the user's daily energy needs. Buildup of dust particles over the PV array reduces the array output, the extent of which depends on the physical location of the array e.g. can be high around the city caused by car pollution and dust in the air, in the coastal region salt can buildup on the array surface due to long period of no rain.

Abdul-Aziz and others [11] conducted research on the impact of shading on a Yingli YL250P29 PV module and concluded that reduction of irradiation because of module shading affected the output of the PV module. The module voltage changes when a shadow occurs. In a string of series connected cells in a module, current flowing through them is the same. By shading one cell, the maximum current is reduced, and this decreases the output power of the PV module. The shaded cell develops a high

temperature, which can destroy it leading to a phenomenon called ‘hotspot’ or damage to the PV module.

Aging of the solar module during its operation is a major derating factor as some array capacity is gradually lost over time. The manufacturer’s warranty specifies this degradation factor as below 15% for the 25-year warranty period of a PV module.

2.2.6 Components of a Solar PV System

Different components make up a solar PV system besides the PV modules. Understanding the function of different components for successful planning is necessary. A simple PV system may consist of a PV module and a load. With increase in load demand, the system becomes more complicated and requires additional components like a backup storage device to store PV power generated for use during the night or during poor weather day. A power converter that converts the DC voltage from the PV module to AC voltage required by connected AC loads and other components for power control may also be required.

Solar PV system can be grouped into three main configurations or types as stand-alone, grid-tied and hybrid with the basic photovoltaic principle remaining the same. The stand-alone configuration relies on the sun only. They may consist of a solar PV module and load only or incorporate energy storage system to operate in the absence of sunlight. Grid-tied on the other hand may consists of a solar module connected to utility grid and load while a hybrid system consists of a solar module, energy storage system, grid and load. The required components depend on the method of configuration used i.e. whether the system operates as a standalone, grid-connected or

hybrid. The study conducted in [12] identified the most important components in a PV system as solar PV module, mounting structure, energy storage system, DC-DC converters, DC-AC inverters, cables and load. During the planning phase of a PV system design, only the load is important while the components of solar PV are considered as PV modules.

2.2.7 Location Issues

The inclination of a PV module changes the reception of the energy on the surface of the PV module. When the module faces the sun, the amount of received solar energy is increased. The effect of inclination on a solar PV module shown in figure 2.2.

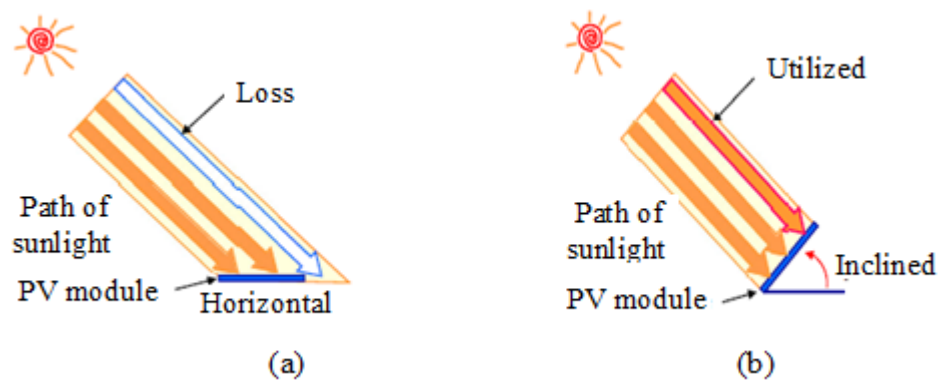


Figure 2.2: Effect of inclination on a PV module

The angle of inclination is optimized by taking climatic conditions and latitude into account. A solar PV module can be mounted on a tilted array frame to fix it at a preferred angle or mounted flat on a rooftop raised parallel to the roof to avoid additional cost of optimization. Others may be mounted on a pole. For better performance all the year round, the modules should be mounted facing optimal orientation or azimuth. True South in the northern hemisphere and True North in the

southern hemisphere are the optimal tilt directions of installing solar PV modules. This means that the modules must be mounted facing the equator. Research conducted in [13] show that decreasing the tilt angle of the PV module from the optimal case 34.5° to 0° decreased the module output power by 13.7%. More losses result by changing the module orientation away from the optimal tilt angle. It is worth noting that the module output drops faster than its gains with every tilt from optimal case.

2.3 Energy Storage System

Due to the intermittence nature of solar energy, there is need to store surplus generation for use during the night or poor weather. Battery Energy Storage System (BESS) are generally used for storing the surplus energy. Traditionally the battery refers to any storage device producing DC power. In recent years, some integral devices have been included to enable the energy storage device to operate e.g. pumping system, integral battery management and protection devices. Battery energy storage system in this study will comprise the battery and associated components like inverters for conversion of DC to AC. The BESS can be charged either from the grid electricity or from the PV module while discharges to the load at different time may depend on the system function. Batteries store electricity, they do not generate electricity like solar PV and wind generating systems. Theoretically, the maintenance of a battery is very easy since it need no mechanical maintenance such as lubrication or overhaul required.

2.3.1 Battery Types

Primary batteries are those that cannot be recharged during their normal operation while secondary batteries can be recharged. The secondary batteries are preferred because of their long life and high energy densities [14]. The primary battery produces instant current upon its installation and are usually very small and portable while having higher energy density compared to rechargeable type of same capacity. The battery manufacturers recommend that it is disposed when used up since its chemical reactions are not reversible and thus cannot be recharged. This feature makes the primary battery unsuitable for use in photovoltaic system. Examples of primary batteries are carbon zinc, and alkaline batteries.

The secondary battery also known as secondary cell or rechargeable battery are assembled with active substances during its manufacturing. This type of battery is recharged by applying suitable external voltage rated for the purpose and reverses the chemical reaction that occurs during its time of discharge to their initial conditions. Lead acid is the oldest form of rechargeable battery used in automotive and boat industry. Other forms of secondary battery are Dry Cells including Nickel-zinc (NiZn), Nickel-cadmium (NiCd), Nickel-metal hydride (NiMH), Nickel-zinc (NiZn), and Lithium-ion (Li-ion). Popular secondary battery storage of Lead acid and Li-ion types are used in solar PV systems and their details are discussed in section that follows.

2.3.1.1 Lead-Acid Batteries

The main contents of a Lead–acid battery are metallic lead (Pb), lead oxide (PbO₂), and sulfuric acid (H₂SO₄) [15]. Lead oxide in various compositions make up the positive electrode. The metallic lead containing small fractions of tin, calcium or antimony makes up the negative electrode. Concentrated sulfuric acid with acid concentration about 35%–40% with the remaining percentage mainly water used as electrolyte. The technology uses liquid electrolyte contained in an airtight upright container. Lead-Acid battery is a rechargeable battery available since its invention by French physicist Gaston Planté in 1859. Its power-to-weight ratio is large and costs less as compared to other rechargeable batteries making it more attractive for high current supply as in photovoltaic system. Because of its reliability and cost, it has remained around for long. Its high current supply and low manufacturing cost makes it popular. It is the most cost effective technology among rechargeable batteries and can be recycled or disposed of easily. A bigger portion of the world’s overall lead production goes to battery manufacturing.

Electrical energy is stored in the battery in form of chemical energy and the stored chemical energy is converted back to electrical energy. The process of converting the electrical energy for storage as chemical energy is referred to as ‘charging’ the battery whereas the process of converting back the stored chemical energy into electrical energy to supply the external load is referred to as ‘discharging’ the battery. The battery acts as an energy source when discharging. A typical lead-acid battery is represented in figure 2.3.

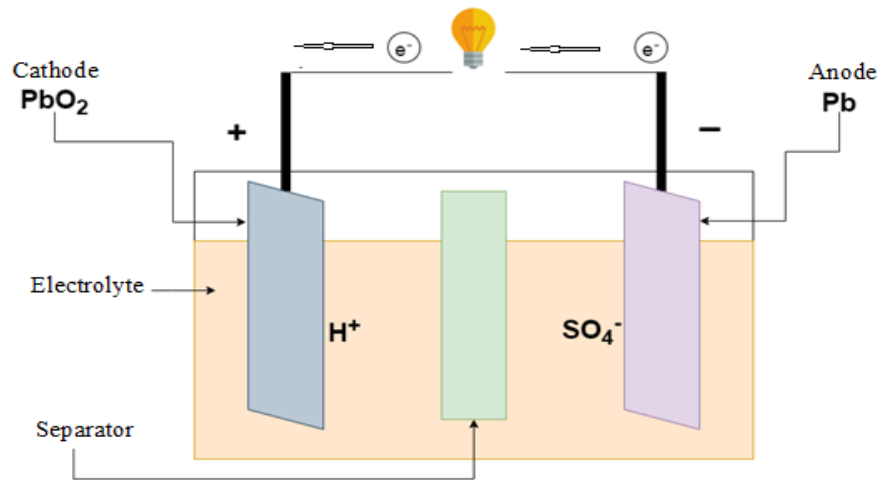


Figure 2.3: Lead-acid battery discharge mode

On discharging the battery, the electrolyte (dilute sulfuric acid) H_2SO_4 breaks down into hydrogen ions and sulfate ions. The hydrogen ion takes an electron from the positive electrode and the sulfate ion gives an electron to the negative plate. The current flows through the external load circuit due to the inequality of electrons to balance the inequality of electrons.

The lead-acid batteries used in solar PV system are grouped as flooded (wet cell), maintenance free (liquid) and maintenance free (Gel).

The flooded type has its liquid (distilled water) topped up frequently because it loses hydrogen over time, is durable, relatively strong against overcharge, readily available and has wide range of capacity up to about 2000 Ah, 2 V unit. These batteries are the most used type in the market.

The maintenance free (liquid) is easy to handle, readily available in the market, weak against overcharge, limited range of capacity up to 150 Ah recommended for small applications, and needs good charge controller to avoid overcharge.

The maintenance free (Gel) is permanently sealed uses silica to convert its electrolyte into jelly like substance. It is easy to handle, weak against overcharge, readily available in the market, recommended for small applications and needs good charge controller to avoid overcharge. Valve regulated Lead-acid battery (VRLA) is a recent improvement of maintenance free (Gel) popular for general industrial use.

The limitations to the lead-acid battery listed; hazardous hydrogen gas vaporizes from electrolyte during the battery-charging period, the battery is sensitive to temperature, which shortens its life, storing the battery unattended for long not recommended because they quickly discharge, the electrolyte used is harmful and protective measures recommended while handling the unsealed battery.

2.3.1.2 Li-ion Batteries

Lithium ions used as electrolytes in a Li-ion battery. Its electrodes can be manufactured from different materials, commonly graphite as the anode and lithium cobalt oxide as the cathode. Lithium iron phosphate or lithium manganese oxide materials also used in the manufacturing of the cathode. Li-ion batteries can deliver large currents for applications requiring high power, their maintenance cost is generally low, scheduled cycling not required for maintaining battery life. At high voltages the battery is liable to damage and a tendency to overheat leading to combustion. Lithium ions (electrolyte) are flammable and can explode if incorrectly charged.

Zhang and others [16] applied Li-ion technology in transport sector to reduce GHG emission from vehicles. The Li-ion battery has high energy density, promising battery

system and light in weight. The current development in the battery manufacturing has its positive electrode manufactured from metal oxide and the negative electrode manufactured from carbon with lithium salt. The manufacturing cost of a Li-ion battery is high compared to other rechargeable batteries of equal capacity. For safe operation of the battery, monitoring circuits are required. The efficiency of the battery is lost even when the battery is not in use.

2.3.2 Battery Management

Battery management involves operating it within the designated safe operating limits, state of charge monitoring through sensors, controlling its condition and adjusting the conditions when necessary in order to enhance its life. The operating conditions to be controlled include current, voltage and power. The State of Charge (SOC) and State of Health (SOH) of the battery are the most important parameters to monitor in the battery management.

2.3.2.1 Battery SOC

The battery SOC is the remaining power of a battery when expressed as a percentage of the rated capacity. If the SOC is 0%, it means that the cells are completely discharged whereas a SOC of 100% means the cells are fully charged. Practically the SOC is maintained above 50%. Lower discharge rate means more energy is available while more discharge current reduces available energy and therefore less discharge current is recommended in order to enjoy more energy. The charge controller controls the charging and discharging of a battery. It protects the battery from overcharge and

over discharge. Overcharge protection stops charging current to avoid further increase of the battery voltage and the function is triggered when the battery voltage reaches the float voltage. Over discharge protection stops discharging current to avoid further decrease of battery voltage and the function is triggered when the battery voltage drops below the Low Voltage Disconnect. The battery SOC is estimated using cost effective Genetic algorithm technique using few number of sensors for a shorter time with the battery terminal voltage and current sensed in the process while the battery is in use.

2.3.2.2 Battery SOH

The Battery SOH is the overall status of the battery. Aging and charging cycles are the main important factors limiting the SOH of a battery. The battery SOH as in [17] is expressed by equation (2.2).

$$SOH = \frac{C_{nominal} - C_{loss}}{C_{nominal}} \quad (2.2)$$

where $C_{nominal}$ and C_{loss} denote the nominal capacity and the capacity loss of the battery respectively. SOH estimation is best done using the cost effective Genetic algorithm technique while the battery is in use.

2.4 Microcontrollers

A microcontroller belongs to the family of microcomputers fabricated on a single chip using VLSI technology governing a specific task in an embedded system. Their architecture and features are discussed in detail component by component. The processor, memory and peripherals are the main components constituting the

microcontroller. The processor is the most crucial component of the microprocessor. The microcontroller is present in control applications to execute a specific function like measurement, controlling, value calculation or display. Areas of application include instrumentation and process control, consumer electronic projects, industrial automation, communication and multimedia applications. The microcontroller receives and interprets data from the input/output peripherals using its central processing unit, stores the temporary information it receives in its data memory and executes the instruction.

2.4.1 Microcontroller Architecture

The Central Processing Unit (CPU), memory, input and output ports (I/O), timers and counters, Analog to Digital Converter (ADC) and Digital to Analog Converter (DAC) constitute the microcontroller architecture [18] as shown in figure 2.4.

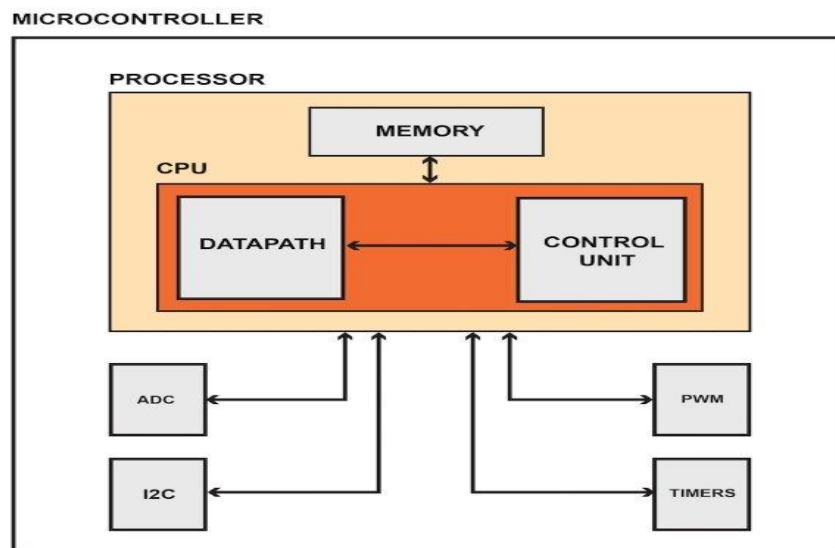


Figure 2.4: Microcontroller architecture

The Central Processing Unit (CPU) consists of Arithmetic Logic Unit (ALU-data path) and a Control Unit. The CPU is the brain of the microcontroller and coordinates the communication between the peripheral devices. The CPU does fetching, decoding and executing the instructions. The ALU performs all the arithmetic and logic operations. The control unit controls the communication and timing between the CPU and the peripherals.

The program memory records and stores all instructions given by the CPU. Both volatile random access memory and the non-volatile read only memory (ROM) are memory housed in the memory. The memory also houses the modern Electrically Erasable Programmable Read-Only Memory (EEPROM) and a certain amount of external memory (flash).

The input and output ports (I/O) are physically connected serial or parallel ports used to interface the microcontroller to the associated peripherals or outside world like external memories, LCDs, LEDs and printers. Sensors are used to interface the input data to the microcontroller. The available ports function as input as well as output port.

Timers and counters are used in frequency generation, pulse generation and clock functions.

The analog to digital converters (ADC) are transducers, which convert analog signals from a sensor output like voltage or current into digital signal number (0 or 1) representing the magnitude of voltage or current that is suitable for the microcontroller

input. Their applications include, but not limited to, scientific instruments, digital signal processing and displaying.

The output of a digital to analog converter (DAC) is an analog signal. It is constructed from discrete electronic components and their applications include, but not limited to communications, actuating a physical system like turning ON or OFF a relay or mechanical switch. Its function is just the reverse of the ADC.

2.4.2 Desirable Features of a Microcontroller

Microcontrollers consume less power, support 1.8 to 5.5 V. Their EEPROMs are storage components capable of technological improvement and hence allowing for more write/erase cycles. The microcontroller together with its integral parts (compact chip) are generally very cheap. The microcontroller chip is reliable and user-friendly processing tool. Despite the disadvantages that may be present, the microcontroller is convenient and useful for control of micro and small devices. A microcontroller is really a small computer. Arduino board is a hardware platform having a microcontroller based on it. Having the Arduino, devices can be designed and built to interact with the surroundings; thus a tool for controlling electronics.

2.4.3 Arduino Microcontroller

Arduino was first introduced at Ivrea Interaction Design Institute in 2005 developed for fast prototyping and its use has become very popular in electronic fields since then.

The microcontroller evolved fast to adapt to changing new needs and challenges. Thousands of complex scientific instruments and projects employ Arduino as the brain over the years. Arduino is an open source electronic building platform consisting of a programmable physical circuit board accompanied by Integrated Development Environment (IDE) software [19]. Arduino boards are capable of reading inputs and turning them into outputs. Examples of the Inputs read by Arduino are like current or voltage signals from sensors. The outputs may be activating or deactivating a relay or turning on a LED. These happen upon sending a set of instructions to the microcontroller through wiring based Arduino programming language and the software based IDE. A number of advantages of using Arduino enumerated as in [20]. Arduino IDE is easy to use (basic electronic knowledge required for beginners) and flexible enough for advanced users. Advanced programming through C++ libraries, published as an open source tool, can extend the software (Language). Extensible hardware for experienced circuit designers are published under the Creative Commons license. Arduino boards, as compared to other microcontroller platforms, are less expensive and can be hand assembled. The software IDE runs across various platforms; Windows, Linux and Macintosh OSX operating systems. Most other microcontrollers operate on windows only. Arduino UNO board is the most popular in Arduino family because its coding is simpler.

2.4.3.1 Arduino Uno Board

Research conducted in [21] listed the different components or parts of Arduino board commonly used in electronic projects as discussed.

The microcontroller, which is the integrated circuit (IC), is the main component in the Arduino board and is slightly different for other types of boards. The specifications of the IC are specified on its top surface and datasheet.

A₀ - A₅ are analog input pins that read analog signals from sensors like current and voltage sensors and convert the signals into digital values the processor can read.

The board has 14 digital pins configured as input pins capable of reading logic values 0 or 1 and output pins which actuate a process e.g. actuating a relay or lighting LEDs.

Ground (GND) pins used to ground the circuit board, several ground pins are available on the board.

The 'reset' button enables resetting of the board or restarting the program from the beginning. The external reset button is connected to the reset pin on the board. The crystal oscillator deals with timing issues by calculating the time. The oscillator has its frequency printed on it e.g. 16 MHz

The LED indicator lights up when Arduino is plugged into a power source as long as the circuit connection is correct, the LED lights up automatically but fails to light up when the connection incorrectly done.

The barrel jack powers the Arduino boards directly from AC power source. The Arduino has an USB connection on its board which can be powered from a PC using a USB cable.

A 16 MHz Arduino Uno board available at Amazon online UK shop is shown in figure 2.5.



Figure 2.5: Arduino Uno board [22]

2.5 Impact of Solar PV System Installation

The impact arising from the solar PV system installed to supply a load demand is classified based on environmental impact, financial impact and social impact. Both positive and negative impacts are cited in the study.

2.5.1 Environmental Impact

Photovoltaic technology does not produce considerable GHG or air pollution during its operation. Using solar energy can have both positive and negative impacts on the environment. Major positive environmental impact of using solar energy is that it reduces the GHG emission into the atmosphere. Research conducted in [23] using a 100 W polycrystalline solar PV module to assess the energy savings and emissions impact are estimated by savings in GHG emission of 0.52 kgCO₂/kWh when the PV module is replaced by the conventional grid electricity.

Use of solar energy drastically reduces the utility grid electricity need. The study conducted by the UK Energy Saving Trust concluded that between 1.3 and 1.6 tons of carbon emission are reduced by an average home in UK using photovoltaic system in one year [24].

The negative environmental impact arising from the use of photovoltaic system arise at the manufacturing stage. A number of hazardous chemicals including nitric acid, sulfuric acid, hydrochloric acid, hydrogen fluoride and acetone are used for cleaning and purifying the semiconductor surface during manufacturing. Inhaling silicon dust is also a major risk facing workers. Heavy metalloids (copper indium gallium selenide) used in manufacturing certain solar panels require special handling during the disposal stage (end of their useful life) of such panels. Robinson and others [25] concluded that further studies are still necessary to establish the negative impacts of PV installation on terrestrial ecosystem and that such system should remain better alternative to fossil fuel.

2.5.2 Financial Impact

Knowledge of PV system cost, solar production resource and value of electricity is necessary for a robust financial analysis. Thorough economic analysis is required for Sound investment decisions. Installation of solar PV system is increasingly common in many countries because of the declining costs of PV system components. Such PV installations require careful consideration with regard to their initial cost, production value, operation and maintenance costs. The return from PV system is driven by the amount of electricity it produces and the return on investment. The number of kWh produced by the solar PV installation and the worth of the kWh dictates the value of a solar PV installation. The installation is viable at higher net value. Solar PV modules are designed to operate over a 25-year warranty period but are degraded by the sun over time. The solar PV manufacturers define the degradation of the modules due to the sun at less than 0.5% a year.

Electricity generation from solar PV system will displace the same quantity of electricity supplied from the utility grid electricity and hence enabling easy calculation of the energy savings accruing from the use of the solar PV. Other factors influencing the value of electricity produced from the solar PV system include energy escalation rate and individual rate structure. Multiple metrics are available for accurate evaluation of the viability of a solar PV project and may include detailed cash flow analysis, simple payback period, net present value and leveled cost of electricity.

The efficiency and cost are the main barriers preventing the photovoltaic system from its adoption worldwide. The payback period or the return on investment is often

overlooked before investing in a project. The shorter the payback period the more attractive the investment becomes and vice versa.

2.5.3 Social Impact

Social aspect is a basic consideration towards setting up any development project in an area. Solar energy considered clean energy resource is helpful in mitigating GHG effect. Proper usage leads to job creation opportunities leading to income development, consumer choice, community development and better health conditions. Technological advancement among researchers in the field of renewable energy is fast growing to cope with the rapid growth in renewable energy technology. Despite the many social benefits, photovoltaic developers still face certain challenges during the installation and operation of the PV system. Gawande and others [26] discussed the challenges concerning the variation in output of the PV plant arising from the intermittence nature of renewable energy sources and the limitations arising from the local population during the land acquisition process.

2.6 Related Literature on Solar Photo-Microgrids

Burning of fossil fuel in the process of energy generation results in GHG emission, mainly CO₂, into the atmosphere. Many countries have prioritized reduction of GHG emission for the last few decades leading to increase in technologies that are more efficient in generation of electrical energy using cleaner methods. Solar power, as one of the primary sources of energy, has been in use as an alternative clean renewable energy source to fossil fuel burning that is cost effective and uses photovoltaic

technology to generate its electricity. By the end of the year 2020, the International Renewable Energy Agency (IRENA) estimated the global total installed capacity of solar PV at 700 GW [27]. IRENA estimated the global installed solar PV capacity growth from the year 2019 to 2020 at 20%. The global growth in solar energy production has been influenced mainly by government incentive policies supporting its development, technological advancements (technical infrastructure and innovation accompanied by reducing cost of solar PV products and increased efficiency) and related economic benefits to the users. The same growth is affected by factors like lack of proper knowledge amongst the consumers about the solar power technology and the penetration of low-quality solar products in the market. The current scenario of installing solar PV system being off grid and grid tied systems with off grid and grid tied mainly applicable to rural areas and large-scale power plants respectively.

Over the past decade, a number of studies have been conducted on microgrid systems with majority concentrating on microgrid modeling, microgrid energy management and their impact (financial, environmental and social) on installing the solar PV system.

Many studies applied mathematical formulations or modeling of microgrid components using various engineering software to represent the actual solar PV physical system. These models are later simulated at various conditions and the actual PV performance determined; this leads to better understanding or further improvement of the PV system studied. The study conducted in [28] applied MATLAB/Simulink software in the modeling of a grid tied solar PV system outlining the PV module characteristics and related component controls. The energy balance between the

renewable energy resource and the utility grid electricity not addressed despite the two sources of energy supplying a three-phase load. Research conducted in [29] modelled and simulated an energy management system in a smart grid with the aim of maintaining energy sustainability in the smart grid. Solar PV, BESS, electric vehicle, utility grid electricity and loads were the main components of the smart grid. The study implemented modeling and simulation only and no real-time implementation was presented.

To improve sustainability and efficiently manage the energy generated by the solar PV system, a low cost (investment wise) control unit in the form of an embedded energy management unit is necessary. Microcontrollers have been applied as embedded energy management control unit to manage the energy balance in smart microgrids. Many researchers have applied Arduino boards as a real world embedded energy management controller to achieve better efficiency and reduction of energy losses in the field of solar PV systems. In Indonesia, researchers applied Arduino microcontroller to program a load management system for a household with view to improve the continuity of solar PV power supply [30]. The study used the capacity of the battery as a reference so that a drop in battery capacity below 10% of rated capacity triggers the microcontroller to switch the source of power supply to the State Electricity Company that is used as a backup. Arduino microcontroller and sensors were applied in [31] to switch between a low priority load and a high priority load during load shading to trip the low priority circuit but the high priority circuit is not tripped. The user accesses voltage, current and power displayed on an LCD display.

The Arduino microcontroller is utilized for operation, decision-making and economic power dispatch in a photovoltaic power generation system [32].

Advancement in information technology across the world has shown improvement in the method of estimating future solar PV power generation using weather forecasting software that is capable of predicting the weather parameters like irradiance, temperature and cloud opacity in a specified geographical region. One such software is the PVsyst photovoltaic software, which gives a comprehensive examination in a PV venture. The PVsyst uses meteorological data resources, PV technology and PV system components. Researchers have applied the software in two broad categories of study i.e. optimal solar power plant design and energy yield estimation. PVsyst simulation software is used to simulate PV power generation for two sites in Saudi Arabia to determine the exact quantity of total solar power generation in a 25-year period [33]. The study was extended to emission reduction guidelines but the actual impact or exact quantity of CO₂ emission reduced in the study was not presented. A solar PV plant modeled using PVsyst to reduce the utility grid electricity using environment-friendly, grid-tied solar PV system at Islamia University of Bahawalpur, Pakistan [34]. The study needed extension to include the impact of environmental conditions on PV modules too. The study conducted in [35] proposed a simple prediction model that could predict solar insolation for one-day ahead. Weather data of the previous day obtained from the area meteorological administration was used to accomplish their next day solar insolation prediction. The prediction results were used to predict solar energy generation helpful for economic dispatch. The study could not forecast energy generation beyond the next day; it required a more accurate prediction

model based forecast for solar parameters. In recent studies, research has shown that API software have been applied in meteorological field to predict future weather pattern for as long as seven days ahead with appreciable accuracy. Bright and others [36] validated Solcast's global performance on an hourly Global horizontal irradiance (GHI) data. The study provided a comprehensive validation highlighting the strengths and weaknesses of the data.

As for any other business, a successful investment follows a feasibility study conducted before commencement of such investment. Investing in renewable energy resource require feasibility study conducted to determine the financial and technological viability of the investment. The study involves conducting a site inspection, preliminary selection of solar components and making basic solar power production estimates. This helps limit the roadblocks associated with the solar PV projects at the beginning of the planning phase and thus limiting the investment risks by addressing the critical design constraints earlier. Without proper feasibility study conducted, solar PV projects may go over budget or likely, to stall. This process is relatively simple for a small project but becomes complex with increase in the size of a project. The risk assessment conducted in [37] before investing in an on-grid solar PV project for green electrification of Cedars hotels shows that there are various alternatives that can be taken to maximize profitability of such projects and that the benefits out ways the risks. Investors of solar PV installation require deeper understanding of financial implications in their installations to enable them calculate the return on investment, reduce financial risk and determine the viability of the project. The economic analysis in a photovoltaic installation is centered on the project

initial cost and the revenue potential of the project. The feasibility study conducted in [38] concluded that installing a grid-tied solar PV system for a home is not financially feasible factoring in the current price of electricity in that region but the investment is less costly than grid-line extension. No on-site survey conducted, no ground-measured data collected, the secondary data used as the solar resource data for the study. The financial impact of installing a solar photovoltaic system for an individual household resident in Germany, Spain and Croatia was assessed in [39]. Despite the low solar radiation and higher electricity prices in Germany than Spain and Croatia, solar PV installation is very profitable in Germany than the other two countries having higher solar radiation.

Solar energy has many economic benefits during its installation and operation. Solar PV incentives offered in form of tax credits by the state can help the photovoltaic developer on reduced fast cost of solar PV products. Solar energy lowers the national grid electricity bill and also results in more job creation in the photovoltaic sector, as more people every year are involved in the design, installation and maintenance due to rapid growth of solar energy across the world. Producing a free power for the 25 years is the average lifespan of the PV module is possible. Going solar reduces the risk of environmental pollution arising because of burning fossil fuel as applied to conventional energy generation process. This is because solar technology does not require combustion of fossil fuel, which releases harmful pollutants into the atmosphere thus lowering the GHG emission into the atmosphere. United States Environmental Protection Agency (EPA) declared CO₂ as the primary greenhouse gas emitted into the atmosphere through human activities [40].

2.7 Current Trends in Microgrid Energy Management

Utility grid electricity is still the biggest supplier of electricity to consumers in Kenya. Other sources rapidly picking up are solar photovoltaic system and wind power with the solar photovoltaic system found to be productive in all parts of the country. Accelerated growth in renewable energy expected in the year 2022 because of concern in support for environmental, climatic change and governance considerations. The rapid rise in energy deployment in photovoltaic sector largely influenced by government incentives on the cost of solar panels and other equipment, technology advancements in solar PV modules and storage batteries. Emerging efficient solar panels in the market enables electricity production in a limited space. Solar shingles are widely spreading than there were ever before despite their stable costs.

Photovoltaic module manufacturers are improving on the warranty period of the modules than ever before attracting many investors into the sector. Advancement in solar inverter technology has led to improvement in PV system efficiency as inverter losses accounting for major losses are minimized. The advancements are good news for photovoltaic developers. Solar powered LED lighting used as streetlights cuts energy bills and GHG emission in many urban areas promoting energy efficiency and protecting public health. Solar power applications are expanding each day as new uses are found and the continued trend opens up new opportunities for photovoltaic developers.

In the near future, the world will solely depend on renewable energy as targets have been set by some countries to become 100% dependable on renewable energy technology in the power sector. Photovoltaic developers are urged to consider solar

batteries for energy storage to reduce possible black outs and power shut off for public safety as was in West Coast, USA done to prevent wild fires. In recent years the capacity has increased while the cost has fallen in advanced solar batteries.

With the growth in transition to clean energy, solar installation service is also on the rise to cope with the rapid growth as many systems require repair and maintenance. Supporting policies like government incentives and net metering on photovoltaic development have witnessed rapid spread of rooftop solar PV systems both at domestic and industrial capacity.

Solar photovoltaic growth is faced with a number of challenges. As many world countries are facing out coal, some countries are still investing in new coal firing plants mostly in developing countries; wealthy countries still fund large amount of coal firing plants in developing countries [41]. Technical knowhow or labor shortage have thwarted the growth in photovoltaic sector. Time taken to train solar installers or employees take long hindering the business expansion. COVID-19 pandemic lead to factory closures and hence raw material shortages and shipping delays which have slowed down the supply chain of solar PV panels and other equipment. The 2020 pandemic lockdown forced many Chinese factories (solar panels and other equipment manufacturing included) to close down with some of them not yet operational to date. Port congestion too contributes to the delay in supply chain of the solar products. The shortage of Silicon element, which is the main material, used in PV cell manufacturing poses a challenge to the manufacturing sector of the photovoltaic cells.

Energy management is a trend linking electrification with the advancement in digital technology to execute processes like optimization and tracking energy usage. The

'management' is helpful for goal achievement in areas like reducing GHG emission and cost savings. However, climate events or severe weather like wildfire causes power outages and therefore require energy management to cope with the situation. Both industrial and domestic electricity consumers are eager to find ways of reducing energy cost. About 48 % of the executive respondents from various industrial companies interviewed by Deloitte 2020 in USA desired to cut energy costs by implementing an energy management system (EMS) [42]. In the same study, the respondents concluded that electricity prices are expected to rise in two years' time. Renewable energy resources such as wind power, solar power and battery storage system are currently penetrating the market at industrial scale and can help industries, other commercial businesses and small scale consumers achieve cost saving, GHG emission reduction targets while increasing resiliency. A Greenfield manufacturing facility also known as 'the Smart Factory' is fast developing by integrating the utility grid with the renewable energy sources. Even without policy incentives, the cost of renewable energy equipment have sharply fallen in recent years outcompeting the conventional energy resources. The incentives make the renewable energy sector more attractive and cuts payback time.

The recent advancement in computer networking and communication technology sector has been utilized to improve energy efficiency and reduce wastage in buildings. Automated control systems are promising technologies applicable to more efficient end use equipment, like lighting, for greater reduction in energy use.

Energy management techniques have been in use for quite some time to reduce the energy use in buildings. Advances in energy management techniques beyond this level

have led to the construction of 'net zero energy buildings' producing the energy and contributing this energy to the utility grid. More distributed energy models (on-site generations and renewable energy sources) are currently available because of advances in the methods of power generation and management. With proper energy management and appropriately sized energy storage devices, the end user decides when to store the energy, when to buy it from the utility grid and when to supply it back to the utility grid based on the load and renewable energy source availability.

Arduino microcontroller and sensors are deployed to implement real-time energy management in various fields including but not limited to engineering, agricultural and instrumentation sectors. A few areas of recent applications of Arduino microcontroller are included in the study. Arduino has been applied in agricultural field to control the flow of water for irrigation where wireless sensors are deployed to monitor the physical or environmental parameters like moisture, temperature and pressure [43]. The alternative method of measuring the amount of solar radiation is achieved with Arduino despite the many sensors available for measuring humidity, temperature, light intensity and other weather parameters. By connecting the ground wire of the PV module to the GND pin of the Arduino board and the live wire to any analog pin (A0-A5) and with the module dimension defined, the solar radiation estimated based on the proportionality of radiation produced and light intensity. Solar radiation is given by power per area of the module.

Arduino microcontroller has been applied to control streetlights in urban centers to reduce wastage or unnecessary usage of lighting as opposed to the earlier methods of control using set time or optical control methods. The modern smart system

incorporating Arduino microcontroller turns ON or OFF lights taking into account the specified intensity of ambient sunlight.

Solar panel performance largely depends on the sun's rays it absorbs. On a sunny day, solar panels supply load power and charge the batteries but on a cloudy weather, the effectiveness of the solar panel reduces, the battery does not charge to its maximum and will disconnect the load before the desirable time. In a solar PV system, the warranty period of solar panels generally last for many years with slight degradation but still PV installations record short life. The short life mainly results from poor energy management between the PV panel, the energy storage system and the load while poor utilization of the storage system causes major failure. Because of the persisting high failure rate of PV system, related research on energy management using advanced technology is needed to optimize the solar PV system following the sun's availability. By doing so, the impact of the energy management system need be considered.

2.8 Summary

This chapter reviewed the theoretical analysis of the solar PV system components, microcontrollers, the impact of installing solar PV system to reduce the fossil fuel contribution to utility grid electricity, the current trends in microgrid energy management and related literature reviewed by various authors.

CHAPTER THREE

METHODOLOGY

3.1 Introduction

This chapter discusses the approach taken to achieve the set specific objectives of the study. Selection criteria for simulation software used in the study discussed. Also discussed in detail are the technical and regulatory requirements for installation of a solar PV plant, microgrid modeling, energy management and the economic and environmental impact resulting from installing the solar PV system. Limitations and assumptions also considered in this section.

3.1.1 Selection of Simulation Software

Engineers and scientists worldwide use MATLAB to analyze and design the systems and products transforming our world. The MATLAB toolbox is the most natural way to express computational mathematics in the world. Built-in graphics make it easy to visualize and gain insights from data. To model and simulate a multi domain physical system, Simscape enables rapid creation of a model's physical system within the Simulink environment. With the Simscape, physical component models can be built based on physical connections that directly integrate with block diagrams and other modeling paradigms. Simulink, integrated with MATLAB, supports system-level design, automatic code generation, simulation and continuous test and verification of embedded systems. It is a block diagram environment for multi domain simulation and Model-Based Design and it exports simulation results to MATLAB for further analysis. Simulink is used to model algorithms, linear and nonlinear physical systems

using block diagrams. With Simulink, the modeled system can be simulated and the results viewed on the scopes and other graphical displays. Configuring the models to run in real time enables the use of hardware-in-the-loop simulation to test the controller. Design changes can be made earlier in the development process and hence reducing costs and shortening the design cycle.

Arduino module is an open source electronic building platform consisting of a programmable physical circuit board and an accompanying software [19]. The Arduino software Integrated Development Environment (IDE) is easy to use for the beginners, advanced programming, extension of the software and also Arduino boards are less expensive compared to other microcontroller platforms. The preassembled Arduino module also costs less and has extensible hardware. The IDE software makes it easy to write code and upload it to the board without connection to the Internet and thus is recommended for users with poor or no internet connection. To use offline IDE, the user only need to download and install the application on a laptop or PC, connect the Arduino board to the device and open the IDE Software. The IDE software runs on Windows, Macintosh OSX, and Linux operating systems. The language is expandable through C++ libraries.

PVsyst photovoltaic software is a software package for the study, sizing and data analysis of complete PV systems. It deals with stand-alone, grid-connected and DC-grid PV systems. It includes extensive PV systems components databases and meteo computations as well as general solar energy tools. The software is helpful for educational training, engineers and architects. The software contains a set of tools to display graphical meteo data that includes irradiation under a clear day model, solar

geometry parameters, PV-array behavior under partial shadings or module mismatch, optimizing tools for orientation and tables. Data can be exported for use in other software. Microsoft Office supports PVsyst software: Up-to-date Windows 7, Windows 8 and Windows 10. The software is preferred for its ability to estimate hourly, monthly and yearly solar energy production numbers with an accuracy of the order of $\pm 5\%$.

The Solcast's API Framework delivers historical, live and forecast solar radiation and PV power data for anywhere on Earth. The API software is hosted in Amazon Web Services offering very robust and scalable method of data exchange to the users. The API Toolkit is a web interface to API services that guides in setting up a forecasting site for accessing worldwide datasets or downloading a given format of historical data. At its core, it provides a simple starting point for accessing live, forecast and historical data services. The Toolkit enables addition or removal of forecast sites, purchase of historical data or share access with other users. In the Toolkit, the user is able to view real-time graphs of live and forecast data at the test site, which changes with each Rapid Update. The Solcast's live and forecast solar data are updated at 30 minute resolution via the API Toolkit. The 'historical data request' section of the API Toolkit allows retrieval of data from up to the last 15 years before the present. The Access to Solcast's API Toolkit is easy and straightforward. Free registration to the API Toolkit is required thereby the user can create own forecast site and download solar data of the study site. No credit card is required and no strings are attached to the free account; the user only needs the API software installed on a networked mobile device like laptop or smart cell phone. The Solcast's historical datasets found to be of good quality

and therefore recommended for use by many researchers. The climate type and the continent or region are the two main inputs for the Solcast's validation tool.

3.1.2 Site Location

The output power of a PV module is approximately proportional to the intensity of sunlight. The site location for solar panel should be such that it is able to capture enough sunlight. The PV efficiency depends on the site of installation of the system, the weather condition and the time of the day. The amount of sunlight reaching the PV module is significantly reduced by shading, therefore it is important to install a solar panel in an open space where it is free from any obstruction or shadow [44]. Orientation is the direction in which a solar panel faces and it affects the amount of sunlight hitting the panel, which eventually affects the module output power. Solar PV modules can be installed on solar trackers to follow the sun but this is very expensive. The common practice generally involve mounting the panels flat on the roof but raised parallel to the roof for ventilation thus taking the slope of the roof. Others are mounted on a tilted frame at a preferred angle or on a pole separate from the house. For a grid-tied PV system, the total power generation and land area are important while maximize annual power generation and minimize the necessary land area. The panel orientation or tilt must consider local weather condition. The minimum tilt angle is 10° - 15° to avoid dust accumulations. The inclination of the PV module changes the reception of solar energy on the surface of the PV module. When the PV module turned towards the sun, the amount of received solar energy is increased. Solar panel generates maximum output when oriented perpendicular to the sun. At true solar noon, the

optimal tilt angle is perpendicular to the Sun's rays. The selected site for the study is favored by various factors recommended for solar PV installation requirements; the site has available space for rooftop mounting of solar PV panels if shadings and dust is avoided, there is ease of access to the site by roads and its proximity to existing utility grid connection point.

This study was conducted at Murang'a University of Technology with specific installation at Electrical Laboratory Block located roughly at the center of the university compound. The university was purposely selected because it is a research Centre with potential researchers. The study specifically addresses a small consumer or a household currently connected to a single-phase utility grid electricity supply. The proposed system is not suitable for locations not supplied with grid electricity.

3.1.3 Data Collection

Primary and secondary data were used to achieve the set objectives of the study. The primary data was obtained from physical measurements of parameters in the study site using both hand-held instruments and simulation software tools. Solar parameters were physically measured for a period of one year accompanied by a number of related simulations to ascertain the weather pattern of the study site.

Both basic and intermediate hand-held research instruments were used in the study site. A clamp meter was used for measuring PV output current under load condition, lux meter (irradiance meter) used for measuring solar irradiance, mercury thermometer used for measuring the ambient temperature of the study site, compass used for locating the optimal tilt directions of installing solar PV modules and AC

power meter used for measuring the connected load power. Software tools used in the study included PVsyst photovoltaic software, which provided historical weather data of the study area for the last one year. The API toolkit provided 7-day weather forecast around the study area. Calibration of the hand-held instruments was observed to ensure approved accuracy standards required to collect the necessary data. The accuracy of the software tools is specified in the software.

Journal articles, conference proceedings, textbooks and web pages were the main sources of secondary data used to review the impact of energy management in a PV based microgrid. Arduino microcontroller used to collect secondary data in form of voltage and current using sensors and ADC to achieve the proposed microgrid EMS.

3.2 Microgrid Modeling

Microgrid mathematical modeling and solar PV system sizing are presented in this section. Modeling software tool used and simulated to represent the real time situation of the modeled system. PV system sizing was done by following electric code of ethics to ensure safety and reliability of the system.

3.2.1 Mathematical Modeling of Microgrid Components

Mathematical modeling equations were used in modeling the PV based microgrid components, and later simulated to represent the real-time results of the modeled system. Modeling of the microgrid components was done in MATLAB/Simulink software and simulated.

3.2.1.1 Solar PV Modeling

A solar cell is a p-n junction fabricated in form of a thin film semiconductor able to convert light energy into DC electricity. The standard design of a solar cell consists of an ideal light generated current source, anti-parallel diode to the light generated current source and internal or intrinsic shunt and series resistances. The ideal model of a solar cell ignores the effect of the internal shunt and series resistances but in reality, it is not possible to overlook these parameters because they affect the output efficiency of the solar cell. In ideal model, the optical and electrical losses diverts the generated current from its ideal characteristics. A more practical equivalent single diode model of a solar cell having both series and shunt resistors shown in figure 3.1.

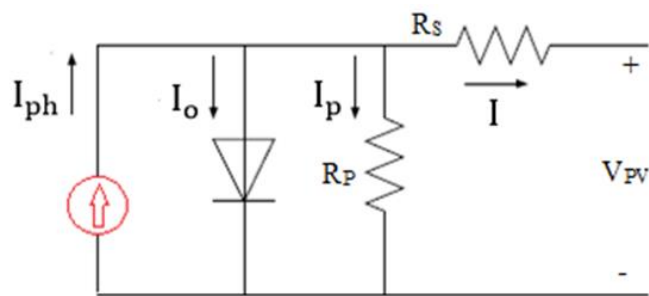


Figure 3.1: Single diode model of a solar cell

By applying Kirchoff's current law to the equivalent circuit, the output current of the solar cell is the balance of photo current, diode current and internal shunt resistance current as in equation (3.1).

$$I = I_{ph} - I_0 - I_p \quad (3.1)$$

where I is the output current of the solar cell, I_{ph} , I_o and I_p are the photocurrent, the diode saturation current influenced by variation in temperature and the current leak in the parallel resistor respectively.

The shunt resistance has an impact on solar cell output current while the series resistance has an impact on the solar cell output voltage. Following these impact, equation (3.1) is modified and expressed as in equation (3.2) [45].

$$I = I_{ph} - I_o \left\{ \exp\left(\frac{qV_d}{nkT}\right) - 1 \right\} - \frac{V + IR_s}{R_p} \quad (3.2)$$

where V and V_d are the actual cell output voltage and the diode voltage respectively, q , n and k are the electron charge, ideality factor of the diode and the Boltzmann constant whose values are 1.602×10^{-19} C, 1.3 and 1.381×10^{-23} J/K respectively, R_s and R_p are the series and shunt resistors respectively while T is the actual cell temperature.

The power output of a PV panel depends on the solar irradiance, area of the PV panel, the panel efficiency and the ambient temperature. The panel output power expressed as [46].

$$P_{pv} = GA\eta \{1 - \gamma(T - 25)\} \quad (3.3)$$

where P_{pv} is the panel output power G , A and η are the solar irradiance, PV module area and the module conversion efficiency respectively, γ and T denote the coefficient of temperature and the ambient temperature in °C respectively. User-defined Simulink model of a solar PV module shown in figure 3.2. Irradiance and temperature specified

as the inputs of the solar PV module. The PV array parameters also specified in the PV array block. The block output parameters are DC voltage and current.

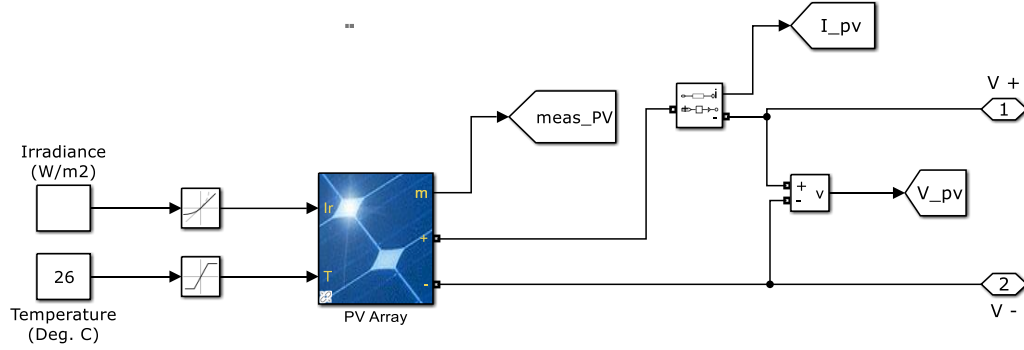


Figure 3.2: Simulink model of a solar PV module

3.2.1.2 Battery Modeling

The battery works as a load when charging and as an energy source when discharging.

The net capacity of a battery in Ah per day expressed as [47].

$$Cb_{net} = \frac{E}{V} \quad (3.4)$$

where Cb_{net} denotes the net capacity of the battery in Ah per day, E and V are the total energy and the system DC operating voltage respectively.

The battery is a charge-dependent voltage source and its state of charge (SOC), which is the remaining power of a battery is expressed as [48].

$$SOC = \left(\frac{Cb_{remaining}}{Cb_{present}} \right) \times 100\% \quad (3.5)$$

where $Cb_{remaining}$ and $Cb_{present}$ denote the remaining capacity and the current maximum capacity in Ah of the battery respectively. Simulink model of a generic lead-acid battery is shown in figure 3.3. The battery input is the DC output from the PV module; its output is also DC voltage. Temperature and aging effects not specified for the Lead-Acid battery.

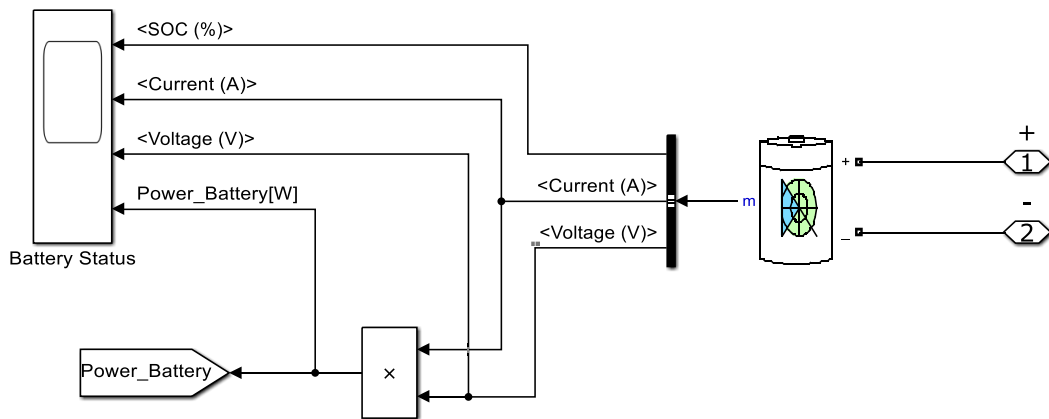


Figure 3.3: Simulink model of a generic lead-acid battery

3.2.1.3 Inverter Modeling

Many appliances use AC power and therefore power generated by DC generating plants converted to AC in order to supply the appliances. A power inverter converts the DC output from both the PV module and the energy storage system into AC in order to supply the rated AC loads. The inverter uses the principle of electronics technology to convert its power from DC to AC. Simulink model of a bridge inverter shown in figure 3.4 is an interfaced user defined, single-phase unidirectional Insulated Gate Bipolar Transistor (IGBT) bridge inverter available in the Simulink library. The

IGBT block implemented a semiconductor device controlled by the gate signal and operated as unidirectional from the PV module and the battery to the AC load with its voltage, phase and frequency harmonized with the grid. The inverter input is the DC output voltage from both the PV module and the battery storage, its output is an AC voltage.

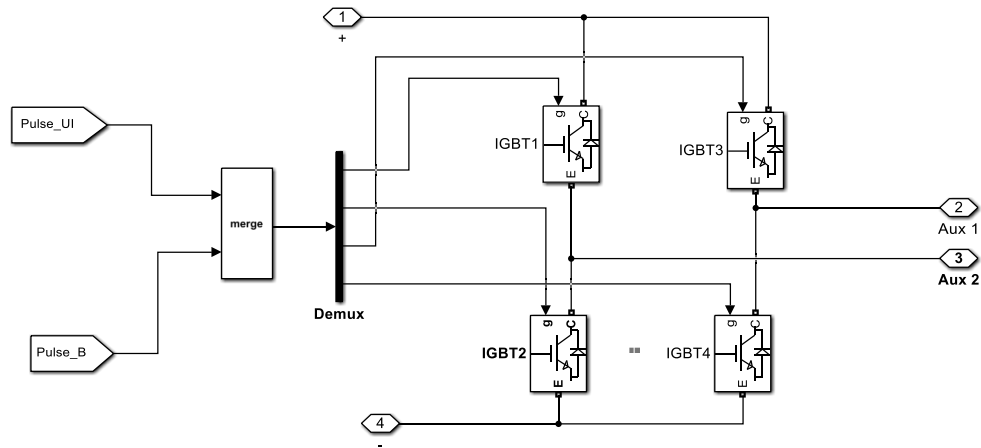


Figure 3.4: Simulink model of a bridge inverter

3.2.1.4 Grid Modeling

The utility grid was modeled as a 240 V single-phase voltage source supplied from a typical 11 kV distribution feeder through 11kV/400V step down transformer. User-defined built-in Simulink model used in the modeling.

3.2.1.5 Energy Management Modeling

The energy management subsystem was modeled to enable energy balance by switching the load between the microgrid sources and the utility grid. PV controller,

battery controller and inverter controller constituted the EMS subsystem model. The PV controller had a preset voltage (V_{ref}), PV module output voltage (V_{PV}) and PV module output current (I_{PV}) as its input. The PID controller implemented discrete-time control algorithms, had advanced features such as external reset, anti-windup, and signal tracking. The PID controller sets the connection from the solar PV module to the load to “ON” on sufficient solar radiation and to “OFF” on insufficient solar radiation. The battery controller sensed the battery voltage (V_{dc}) through signal tracking. This block implemented discrete-time PID control algorithms, advanced features such as external reset, anti-windup and signal tracking. The PID controller sets the connection from the battery to “ON” on discharging and to “OFF” on charging. The battery voltage, utility grid voltage and utility grid current were the input to the inverter controller. The controller implemented a PID controller and a phase locked loop (PLL) system used to synchronize on a variable frequency sinusoidal signal. User defined model by Hiroumi Mita, MathWorks Japan used in the modeling.

3.2.1.6 The Complete Model of the Grid-connected PV System

Both the PV module and the battery storage system connected to supply the load through an inverter to invert their DC output voltages to AC. The load received another power supply from the utility grid via step down transformer. An EMS or control provided to check the balance between the microgrid sources and the utility grid meeting the set threshold limits. The scopes included for monitoring the desired

parameters like voltage, current, power, battery SOC and time. The complete Simulink model of the proposed microgrid is shown in figure 3.5.

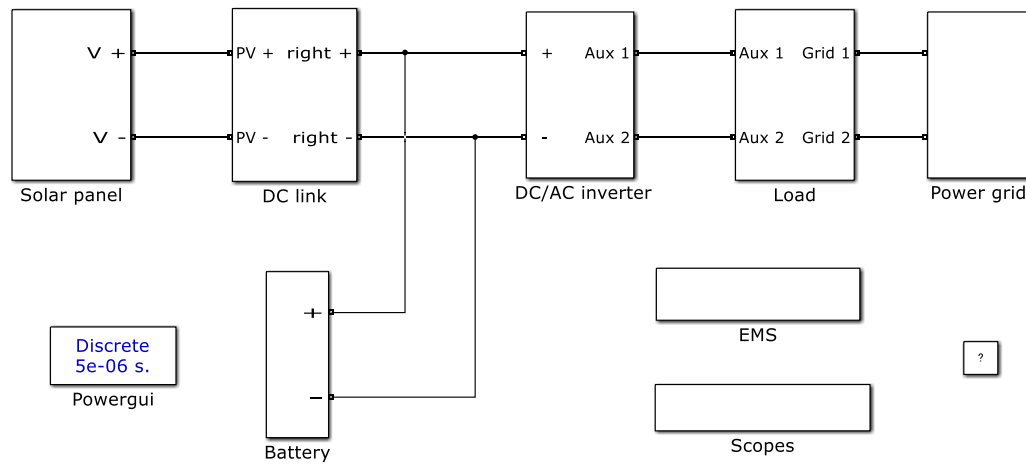


Figure 3.5: Complete microgrid subsystems

3.2.2 Solar PV System Sizing

The PV system sizing considered estimating the consumer load size, determining the required output power of the PV module, sufficient storage capacity of the battery and means of connection to the utility grid via inverter.

3.2.2.1 Load Estimation

Consumer loads in this study were three energy saving bulbs with different ratings and usage as presented in Table 3.1. The bulbs supplied at 240 V, 50 Hz single phase.

Table 3.1 Load Consumption

Loads	Power rating (W)	Quantity	Use/day (hours)	Daily load (kWh)
Load_1	28	1	8	0.224
Load_2	18	1	8	0.144
Load_3	9	1	8	0.072
Total	55			0.44

3.2.2.2 PV Module Sizing

The PV module attachment or support structure used is designed and constructed of a suitable material to resist the action of wind at the site location where the PV system is installed. In sizing the PV module, the total daily load in Watt-hour is determined and the average peak sun-hour of the study area estimated using appropriate software or Google-search. The output power of the PV module is then obtained. Equation (3.6) expresses the maximum output power obtainable from the solar PV module [49].

$$P_{\max} = \frac{E_D}{h} \quad (3.6)$$

where P_{\max} denotes the maximum output power of the PV module, E_D is the daily load in kWh per day and h is the average peak sun hours of the study area.

Using the data obtained from the world weather and climate information [50], the average amount of sun hours of the study area is 2,452 hours a year equivalent to 6.6 sun hours per day. From Table 3.1, equation (3.6) is evaluated and the module output power is 66.7 W. Thus, a standard solar PV module rating of 90 W is required. Yingli solar 90 W panel selected for this study. The electrical characteristics of the panel at STC shown in Table 3.2 and Appendix A.

Table 3.2: Characteristics of Yingli solar PV module

Parameter	Specification	Parameter	Specification
Maximum power	90.0 W	Temp coefficient	38%
Open circuit voltage	22.0 V	Module efficiency	13.5%
Voltage at maximum power point	17.8 V	Panel dimension	1010mmx660mm x25mm
Short circuit current	5.44 A	Warranty	25 years
Current at maximum power point	5.06 A		

3.2.2.3 Battery Storage System Sizing

The battery capacity should be adequate to store excess generation, meet the daily peak demand and supply power for a number of autonomous days on poor weather. The battery life depends on the system voltage, its depth of discharge (DoD), its efficiency and the total daily demand. The minimum battery capacity is expressed by [51].

$$C_B = \frac{E_D}{V \times DoD \times \eta} \quad (3.7)$$

where C_B denotes the minimum battery capacity in Ah, V is the DC system voltage taken to be 12 V, η is the battery efficiency taken to be 85% and the DoD is approximated at 80%. From equation (3.7), the battery capacity is 53.92 Ah thus a standard battery capacity size of 65 Ah is required. Yuasa NP65-12I Industrial VRLA sealed lead, maintenance free, 12 V, 65 Ah battery selected for the study. The selected battery has a nominal voltage of 12 V, 20-hr rate Capacity to 10.5V at 20°C of 65 Ah and operating temperature range of -20°C to 60 °C. Technical datasheet for Yuasa NP65-12I available in Appendix B.

3.2.2.4 Power Inverter Sizing

A power inverter converts the DC electricity from the PV module into AC electricity required by the load to operate. The orientation of the PV module and the inverter performance are key to attainment of optimal PV-inverter sizing. The losses associated with power inverter are due to the voltage drop at the push-pull amplifier, which is the final transistor circuit thus, lowering the inverter output voltage. The inverter sized able to meet the maximum output power of the PV module. The total inverter power as in [52] is given by equation (3.8).

$$P_{Inv} = \frac{E_D}{\eta I} \quad (3.8)$$

where P_{Inv} denotes the total inverter power and ηI is the inverter efficiency.

Using the total daily load as in Table 3.1, the inverter efficiency taken as 80%, equation (3.8) is evaluated and the total inverter power is 69 W. Solarpex solar power inverter Model S-150W is selected for the study. The selected inverter has input voltage of 12 V DC, which matches the battery output voltage range and its output voltage 220VAC/230VAC matches the connected load voltage thus meets the general and particular requirements for inverters used in photovoltaic power systems. The inverter has a nominal AC power output capacity of 150 W with a modified sine wave and a frequency of 50 Hz and provided with an overload and over temperature protection.

3.2.2.5 Charge Controller Sizing

A charge controller is a switching device that protects the batteries from overcharge and over discharge. Overcharge protection is to stop charging current to avoid further increase of the battery voltage. The charge controller disconnects the PV module from the battery to stop charging. Over discharge protection is to stop discharging current to avoid further decrease of the battery voltage when the battery voltage reaches Low Voltage Disconnect.

The charge controller disconnects the load from the battery to stop discharging the battery. The total current through the charge controller considering a safety factor of 1.25 [53] is expressed by equation (3.9).

$$I_{CC} = I_{SC} \times 1.25 \quad (3.9)$$

where I_{CC} and I_{SC} are the total current through the charge controller and the short circuit current of the selected PV module respectively.

From the PV module performance characteristics in Table 3.2, equation (3.9) evaluated and the total current through the charge controller is 6.8 A. Solarmax Solar Charge Controller Battery Intelligent 10A selected for the study. The selected module has a rated charging current of 10A/20A/30A (optional), a working voltage of 12 V, an over voltage protection of 16.5 V, a short circuit or overload capacity of 1.25 times the rated current and operating temperature range of -35 to 50 °C.

3.3 Real-time Energy Management of the Microgrid

Experimental set up was developed to demonstrate the real-time energy management of the microgrid. In this energy management system, the load supplied from either the solar PV system (PV module and battery storage system) or the national utility grid electricity.

There were various tasks performed to make the microgrid energy management accurate. The first one being monitoring the flow of current to and from the battery bank. The second is measuring the battery state of charge, conducting logical decision making process of integrating the PV module and the battery bank to the external utility grid and the fourth one being synchronization of the renewable energy sources with the utility grid with respect to voltage and frequency.

The proposed energy management was such that solar PV became the primary source of electric supply to the load; the excess PV power charged the battery through the charge controller. With a drop in solar radiation due to drop in irradiance, the battery bank (if it was full) served the load and with a further decrease in battery current beyond a specified limit, the load was supplied from the state electricity grid which was the backup source. The prototype used Arduino Uno microcontroller to program the switching between the microgrid sources and the state electricity grid while meeting the specified thresh hold limits. The load management system used sensors to measure the flow of currents and displayed them on an LCD display for monitoring. The relay interface boards connected the load to the two sources of supplies. Figure 3.6 shows the schematic diagram of the proposed energy management system.

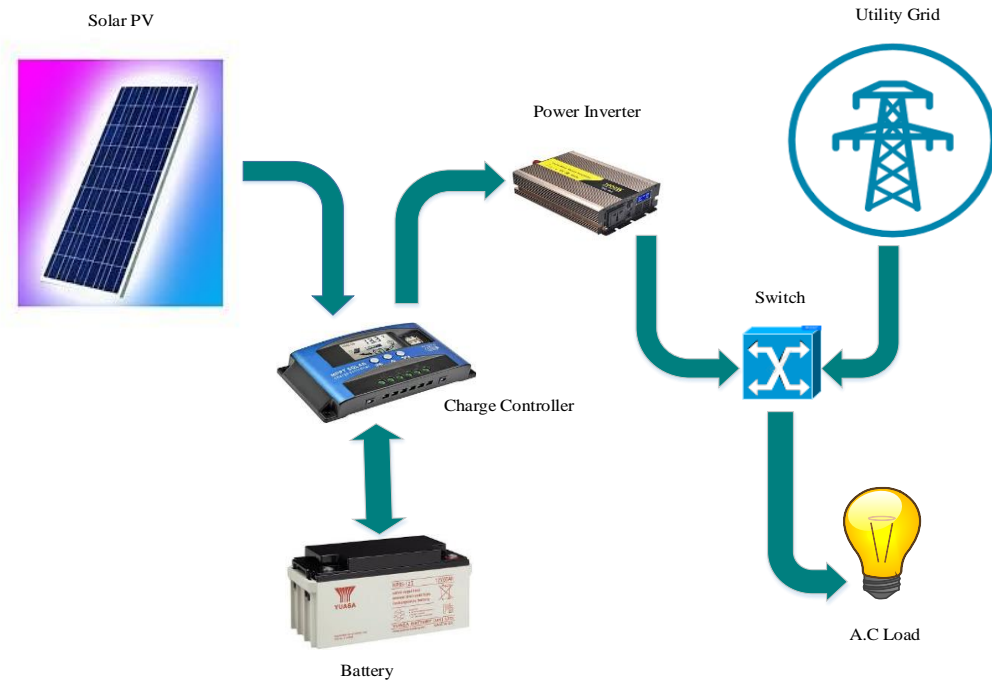


Figure 3.6: Proposed microgrid energy management system [54], [55].

3.3.1 Hardware Implementation

Arduino Uno development board, voltage sensor detection module, current sensor ACS712 (5A), two 8-channel Arduino-compatible AC250V 10A DC12V relay interface boards, 16x2 LCD display and LEDs were the main hardware players controlling the prototype. Arduino Uno development board has 14 digital input/output pins D₀-D₁₃ representing voltages in bits of 1 or 0 (ON or OFF) and 6 analog input pins A₀-A₅ having capability to read analog voltages 0-240 V which are converted to digital signals by ADC. The module was supplied through a USB interface or an external power supply. One LED was used for power indicator, LED 13 connected to

digital pin 13 and indicated the status of the pin i.e. the LED is ON when the pin is HIGH and OFF when the pin is LOW.

Arduino Uno received input from sensors and affected its surrounding by controlling actuators, which performed actions. It consists of two parts i.e. a programmable physical circuit board (microcontroller based on wiring) accompanied by Integrated Development Environment (based on processing) software. The technical specifications of Arduino Uno provided in Appendix D1 and D2.

The accuracy of this energy management largely depended on the performance of the ACS712 current sensor, which detected the flow of current in the circuit. The sensor selected because of its reliability, low first cost, easily interfaced with Arduino microcontrollers, precise in measuring current values and can be installed on an existing installation. It is based on Hall Effect and its output is an analog voltage proportional to the current being sensed. The sensor datasheet provided in Appendix E.

The relay is an electronic switch, which is turned ON or OFF to enable the current to flow or not, controlled by Arduino at low 12 V DC voltage as provided by the Arduino pins. High voltage side was supplied by 240V AC. The relay configurations are normally closed or open. At closed status, current can flow through the circuit but in open status, the circuit is broken and no current can flow through it. The interface directly connected to the microcontroller to enable switching the loads between the two power sources. Figure 3.7 shows the prototype of the proposed microgrid.

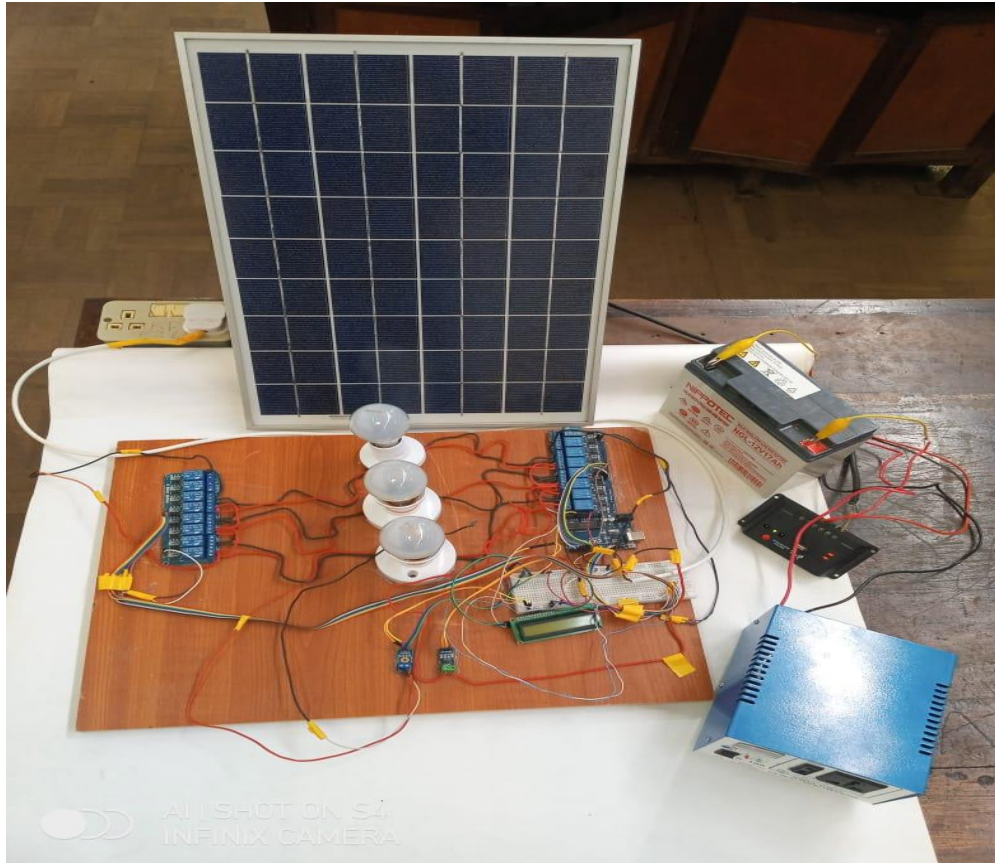


Figure 3.7: Microgrid experimental set up

3.3.2 Software Algorithm

The program was initialized by declaration of variables; the sensors and the modules used in the study. Every module/sensor was assigned digital /analog pins from the microcontroller i.e. `int solarlive1=2;` relay one which controls load_1 is connected to digital pin 2 of the microcontroller. The proposed energy management consisted of three loads represented as load_1, load_2 and load_3 with each load utilizing 4-channel relay, two relays for the solar PV system and two other relays for utility grid electricity. Relays for load_1 are identified as `solarlive1`; `solarneutral1`; `gridlive11`;

gridneutral1. The configuration ensures complete isolation during switching. The remaining loads follow the same identification code and sequence.

Libraries are also available in section i.e. OneWire.h and LiquidCrystal_I2C.h. The libraries provide extra functionality for use in the sketches working with the hardware or manipulating data.

Setup () function is called when a sketch starts to initialize the variables and pin modes (input or output) which start using libraries etc. The setup function will only run once, after each power up or reset of the Arduino board.

In this EMS, all relay channels act as outputs because they receive signals from current and voltage sensors to control the switching. The bulk of the Arduino sketch executed in the Void loop (). The loop () function will run repeatedly until the microcontroller is reset. The Void loop contains logical statements used by the microcontroller to determine the set conditions for the loads isolation.

Conditional statements check whether a programmed specified Boolean condition is true or false. Figure 3.8 shows the proposed energy management flow chart algorithm, the conditions are the values of current from the current sensor e.g. if (current >0.12 &¤t <0.22) {relays 1, 2, 7, 8, 11 and 12 are HIGH and relays 3, 4, 5, 6, 9 and 10 are LOW. This disconnects load_1 from the PV system reconnecting it to the utility grid supply. The Arduino code used for the program execution is provided in Appendix D3.

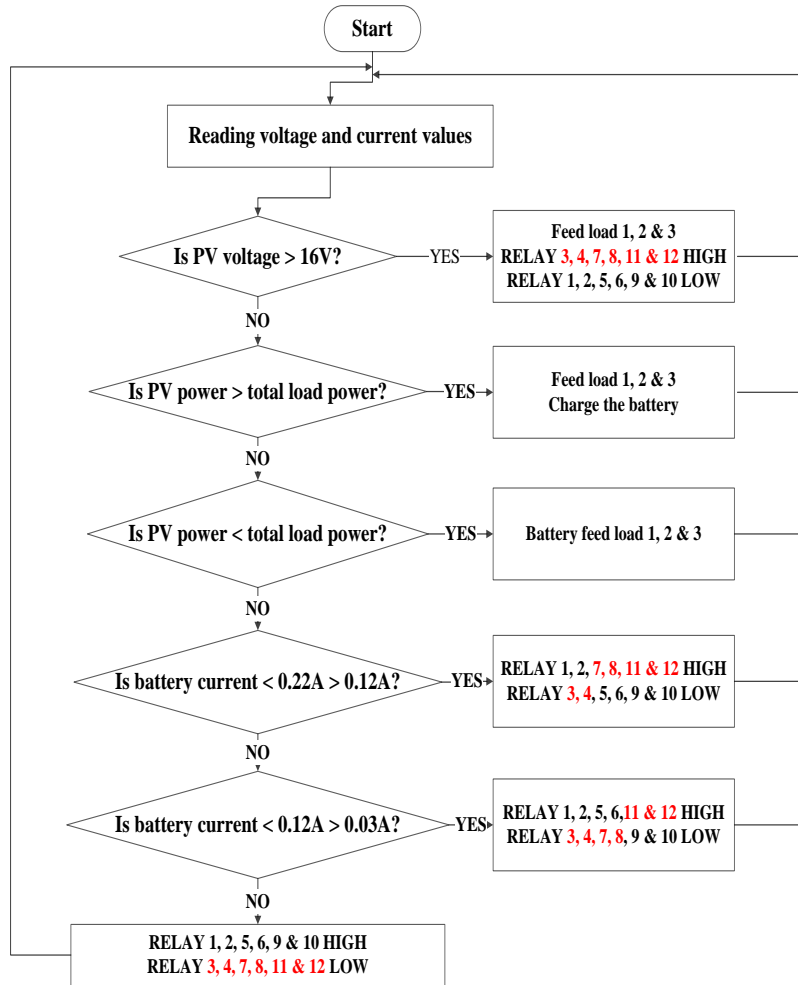


Figure 3.8: Energy management flow chart algorithm

3.4 Estimation of Future Solar Power Production

About 70% of sun's energy reaches the earth's surface; the remaining percentage is absorbed or reflected in the atmosphere [56]. Places near equator receive a maximum solar irradiation about 1,1 kW/m². The intensity of solar radiation determines the amount of energy a solar panel generates, generation is high at higher irradiation and lower at lower irradiation. Irradiance is the amount of solar energy incident on a

specific area for a set time expressed in kWh/m²/day. In other words, it is the amount of solar energy hitting a specific area each day. Murang'a University of Technology is located close to equator with annual average irradiation of 5.07 kWh/m² /day according to PVsyst software on Global horizontal plane, an attracting feature for PV power generation in the study site.

The power generated by the solar PV module in a single day [57] is expressed by equation (3.10).

$$E_g = G \times \eta_{PV} \times A \quad (3.10)$$

where E_g denotes the power generated by the solar PV module in kWh per day, G denotes the irradiance in kWh/m² per day, η_{PV} is the percentage module efficiency and A is the module area in square meters.

3.4.1 Medium-term Weather Forecast

This study used historical meteorological data collected from PVsyst photovoltaic software for medium term weather forecast. Ground measured data, manually carried out at the study site, used as verification procedures for the historical results. Irradiance and temperature are the main variables manually measured by hand held instruments at the study site.

The PVsyst photovoltaic software installed on a networked mobile device provided historical data of a meteorological region for the past one year. Subscription to this software is required; free registration or accounts are rare. After subscription, the user initially browses at “tools” in the toolbox for background data management and

didactic tools, meteorological data (importation from diverse sources and synthetic generation). The user navigates to “solar toolbox” and selects “monthly meteo computation”, thereafter navigates to select the country (Kenya selected for this study), study site (Nairobi selected) taking into account transposition on a tilted plane (tilt angle 30°) and units (kWh/m² per day selected for the study). Quick meteo computations in monthly values that include Global on horizontal plane and Global on tilted plane displayed in table, graphical or printable formats.

3.4.2 Short-term Weather Forecast

The API provides live and forecast solar radiation data around the world using proprietary cloud detection, aerosol tracking and prediction algorithms. The data updated every 5-15 minutes with each new satellite image. Forecast solar radiation data is available for seven days ahead. The Solar Radiation Sites with 30-minute resolution is suitable for users having an application with fixed locations while the built-in accuracy assessment is available in the API Toolkit.

To access the Solcast’s world solar radiation data, the first time user need to register by creating a free API toolkit account followed by creating a solar radiation site and exploring data in the already created site using helpful widgets. A student or a public researcher has access to solar irradiance data only in all locations, free historical data credits (US\$ 650 up to US\$ 5,000), 10 API requests per day and no commercial use license. Once registered, the user browses internet on a networked mobile device like laptop or smart cell phone (having the application installed) at <https://solcast.com>. The user logs in and navigates to the “World API-Radiation” which provides solar

radiation data based on longitude and latitude of the site at 30 minute resolution. Click “Try the world API”, address search for site (Murang,a University of Technology is at longitude 37.147444 and lattitude -0.71566), click the default graph, “Download Data”, select “Forecasts” and finally download data in CSV format. Results of solar radiation data is available in both graphical and Microsoft Excel spread sheet. Desired data variables for downloads include Global Horizontal Irradiance (GHI), Direct Normal Irradiance (DNI), air temperature, zennith, azimuth and cloud opacity.

3.5 Validation of the Proposed EMS

In this section, the economic, social and environmental impact of installing rooftop solar PV system is extensively studied. Economic analysis of a project helps to ensure allocation of scarce resources efficiently while investment brings benefit to the developer.

3.5.1 Cost Analysis

A cost analysis must be done to evaluate the economic option before investing in a solar PV system and the most economical alternative chosen. Investing in a solar PV system is a major investment that influences the future profitability of the investment. The major goal being maximum return on the investment by balancing the ratio between performance and cost.

Direct capital costs are costs assigned to a specific piece of equipment related to the project. The direct capital costs are included in the total system cost or the upfront cost incurred at year zero and includes the PV module, battery backup, inverter, charge

controller, microcontroller and its accessories for this study. Other costs are engineering and labor costs, site acquisition and preparation (absent in this study).

The operation and maintenance costs are costs representing the ongoing annual expenses required to service, maintain or replace components in a solar PV system.

Various components in the PV installation have different life expectancy; some may get damaged during their normal operation calling for immediate replacement.

The total cost of utility grid electricity for a specified period without using solar PV system connection as in [58] is expressed by equation (3.11).

$$C_{grid} = E_D \times C_{units} \times T \times 365 \quad (3.11)$$

where C_{grid} is the total cost of utility grid electricity for the project life, E_D is the energy demand in kWh per day, C_{units} denotes the per unit cost of energy charged by the national utility provider and T denotes the project life time in years.

The total cost of installation of a rooftop solar PV system with no subsidy calculated as in [58] is given by equation (3.12).

$$C_{PVS} = C_{PV} + C_{inv} + C_{bat} + C_{cc} + C_{others} \quad (3.12)$$

where C_{PVS} is the total cost of solar PV system with no subsidy, C_{PV} , C_{inv} , C_{bat} and C_{cc} denote the cost of solar PV panel, power inverter, battery storage system and solar charge controller respectively. C_{others} denote other system capital costs arising from installation (engineering and labor costs), operation and maintenance of the solar PV system. The researcher assumes that the project is 100% funded by debt since there is no known capital investment in it. The renewable energy components sourced both locally and internationally through online shops where appropriate components are

unavailable in the local market. The components and other costs estimates shown in Table 3.3.

Table 3.3: Component and other costs estimate

Item Description	Quantity	Unit price	Total US\$
Yingli solar 90 W panel	1	76.99	76.99
Yuasa 12 V, 65 Ah lead-acid battery	1	70.42	70.42
Solarpex 12 V/230 V inverter	1	19.37	19.37
Solarmax charge controller 10 A	1	23.76	23.76
Arduino Uno & accessories	1	37.85	37.85
Engineering and labor costs	1	57.04	57.04
Total			286

The capital cost of investment using monocrystalline solar PV panel is 9% higher than polycrystalline solar PV panel, therefore polycrystalline solar PV panel was used in this study.

3.5.2 Payback Period

The payback period (PB) is a measure of how long it will be before the investment recovers itself or the number of years required to recover the initial investment cost. The project becomes attractive when the payback period is shorter than the lifetime of the project. Payback period expressed as in equation (3.13) [59].

$$PB = \frac{C_{PVS}}{E_D C_{units} \times 365} \quad (3.13)$$

3.5.3 Net Present Value

The net present value (*NPV*) is critical for determination of economic feasibility of an investment. It calculates the capital costs and net savings incurred throughout the project life and sums them. Savings are represented as positive values whereas costs are negative values. When the *NPV* is positive, the project is feasible and thus acceptable. *NPV* of a project is expressed as in equation (3.14) [59]. The method is used to analyze the project profitability.

$$NPV = -C_{Initial} + \sum_{t=1}^N \left\{ \frac{EC_t}{(1+k)^t} \right\} \quad (3.14)$$

where $C_{Initial}$ denotes the initial cost of investment of the solar PV system with no subsidy, EC_t denotes the energy cost for year t , N is the total project duration period in years, k and t are the discount rate and the year variable in each summation respectively.

3.6 Summary

This section presented solar PV system modeling, PV system sizing, real time energy management of the modelled microgrid system using hardware prototyping, weather forecasting using API and PVsyst photovoltaic software and demonstrated the economic and environmental impact of photovoltaic installation.

CHAPTER FOUR

RESULTS AND DISCUSSION

4.1 Introduction

This chapter presented the results obtained following the methodology adopted to achieve the set specific objectives of the study. The results of the mathematical modeling of the PV-based microgrid, real-time energy management, impact of energy management and weather forecasting of the study site presented and discussed in detail.

4.2 Results of Modeling and Simulation

The connected load of 54 W supplied from two sources of energy i.e. the microgrid source consisting of a solar photovoltaic module and the battery and the utility grid electricity. The output of the solar PV module and the battery are 12 V DC voltages converted to 230 V AC voltage by the power inverter and synchronized to the utility grid voltage 230 V AC before being supplied to the load at 230 V AC so that the connected load receives the same voltage from both the sources. The solar PV module supplies the load on sufficient irradiance and charges the battery with surplus power. With a drop in irradiance, the battery picks up and supplies the load to its discharge level when the utility grid picks up. This process enabled by the EMS subsystem created for the purpose.

The microgrid model of figure 3.5 simulated in MATLAB/Simulink software with the Simulink solver parameter configuration set to discrete to enable faster speed of simulation of the model. The model simulated at average irradiance of 593.31 W/m²

and air temperature of 25.48°C taken from the 7-day API weather forecast taken on 11th March 2022. Irradiance and temperature are the main parameters required for the simulation. The simulation results of the modeled microgrid shown in figure 4.1.

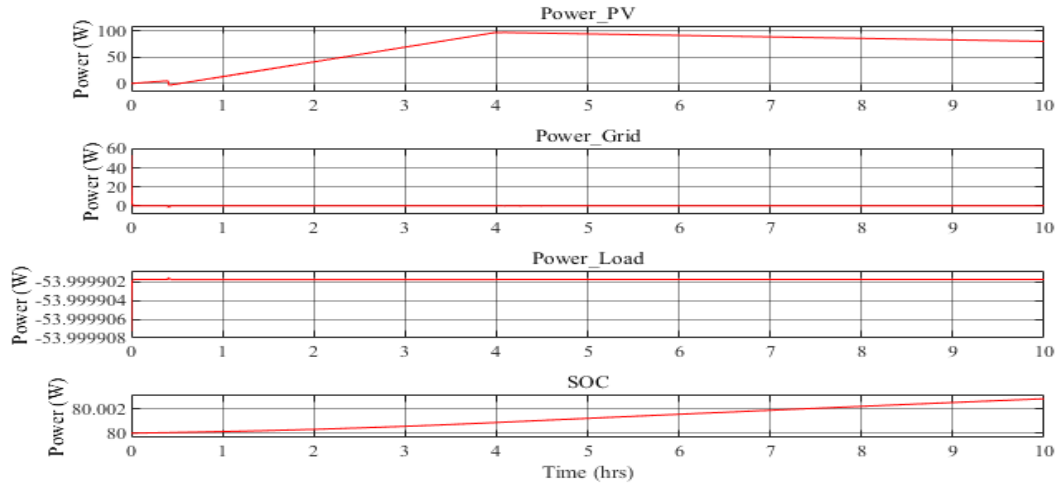


Figure 4.1: Simulated results of power_load, power_PV, power_grid, and battery SOC

From the test results, the connected load had a constant power of 54 W for the simulation time indicated (10 hours). During this period, the connected load supplied from the solar PV power only since the utility grid power remained at zero Watts for the specified time. The PV power gradually rose from a minimum value at zero hour to attain its peak value of 91 W at the fourth hour and linearly drop slightly with decrease in irradiance up to the 10th hour studied. The battery power is seen to increase for the stated time showing that it is continuously charging. For the stated period, the PV power was still sufficient to supply the rated load until a drop in irradiance was experienced to alter the situation, which is the time beyond the simulation time specified as expected during the night.

4.3 Real-time Energy Management

The assembled prototype shown in figure 3.7 operated the connected loads over a 24-hour period starting from 9.00 HRS to ascertain the effectiveness of the proposed energy management system. The loads first supplied from the micro sources (solar PV and battery storage) during the day but the micro sources disconnected after some time at night and reconnected to the utility grid one at a time starting with the highest rated load. This happened because the microcontroller, through current sensors and relays, disconnected the loads following the specified threshold limits set in the energy flow chart algorithm shown in figure 8 reconnecting them to the utility grid. The LCD displayed the source of power supply connected to each particular connected load for the user. 'CONFIGURATING' displayed on the LCD screen upon total disconnection of all connected loads from the microgrid sources to the utility grid. With this configuration, the microcontroller checks the restoration status of the open circuit voltage of the PV module. If restored, the microcontroller switches the loads back to the priority power source. The observation made in this prototype is that the current sensor gave out current values above 0.1 A even at the time of total disconnection of microgrid sources. This is the value used for setting the microcontroller to switch off micro sources reconnecting all the loads to the utility grid allowing for servicing.

4.4 Weather Forecasting

The simulation results of the PVsyst photovoltaic software used as solar resource data for the study area (Nairobi) during the year 2021 is shown in Table 4.1. From the

table, July had the least solar irradiation of 3.81 kWh/m²/day on global horizontal plane; the month of February recorded the highest irradiation of 6.07 kWh/m²/day. The average GHI for the year was 5.07 kWh/m²/day. The average Global on tilted plane for the year was 4.48 kWh/m²/day. The lowest irradiation per month is helpful in sizing the battery capacity of a solar PV system during design time.

Table 4.1 Monthly Global irradiance (Nairobi)

Monthly meteo at Nairobi, (Lat. 1.2°S, long. 36.5°E, alt. 1640 m)
Plane: tilt 30°, azimuth 0°, bo (IAM)=0.05

	Horiz. Glob kWh/m ² .day	Tilted Glob kWh/m ² .day
January	5.97	4.16
February	6.07	4.75
March	5.97	5.27
April	5.13	5.08
May	4.61	4.92
June	4.07	4.43
July	3.81	4.04
August	4.06	4.11
September	5.03	4.71
October	5.48	4.57
November	5.23	3.94
December	5.52	3.81
Year	5.07	4.48

Legends: Horiz. Glob Global on horizontal plane
Tilted Glob Global on tilted plane

Based on Table 4.1, the maximum amount of solar energy generated during each month was estimated using equation (3.10). At a specified irradiance, with the knowledge of PV module efficiency and surface area, equation (3.10) was evaluated using the values in Tables 3.2 and 4.1 to give the maximum energy generated from the solar PV module.

The maximum amount of solar energy generated during the months of February and July were 18.0 kWh and 10.2 kWh representing the months with the highest and lowest PV power generation at the study site respectively. The site's average insolation for different months was also available for further analysis. The knowledge of the amount of energy generated from the solar PV module in each month of the previous year can be used to forecast the PV power generation for the next year assuming no diverse weather changes occurred in the past few years.

Forecasts generally predict what is likely to occur. The prediction contains uncertainty due to the chaotic nature of the atmosphere. The Solcast's probability around the median forecast is 10% and 90% represented as P10/P90 in figure 4.2. The data represented in the figure were obtained from the API live and forecast solar resource data of the study area taken on 11th March 2022 at local time zone, Nairobi 2022-03-11T12:30:00Z. The results show that there were thin clouds persisting reducing the intensity of sunlight at the time of forecast specified. The API weather parameters in the study site summarized in Table 4.2, detailed forecast data, based on satellite images, available in excel spreadsheet found in Appendix F1-F7.

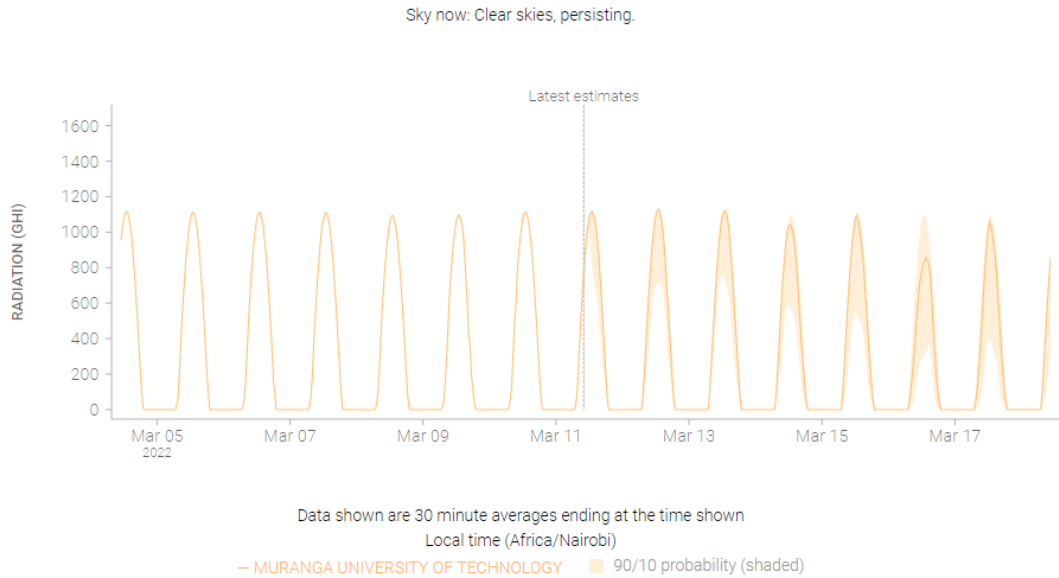


Figure 4.2: Forecast Global irradiance (Murang’a), March 11th through 17th.

Table 4.2: Summary of GHI and temperature, (Murang’a), March 12th through 17th

Day	3/12/2022	3/13/2022	3/14/2022	3/15/2022	3/16/2022	3/17/2022	Average
W/m ²	674.17	665.25	596.66	618.08	467.67	538	593.31
Wh/m ²	8,090	7,983	7,160	7,417	5,612	6,456	7,119.66
Temp °C	26.00	26.58	25.33	25.80	24.92	24.25	25.48

Based on figure 4.2, for the 7-day forecast, irradiance remained near zero during the night but was high during the day with peak value about 1000 W/m². The absence of sunlight during the night contributes to the low irradiance recorded for the forecasted days. From Table 4.2, the maximum GHI of 8,090 Wh/m² per day recorded on 12th March 2022 and the minimum value of 5,612 Wh/m² per day recorded on 16th March 2022. The site’s average GHI for the forecasted days is 7,119.66 Wh/m² per day.

With the knowledge of site irradiance and PV module parameters, equation (3.10) is evaluated and the PV power generated each day forecasted. The forecasted PV power

generated on 12th March 2022 and 16th March 2022 is 720.82 Wh and 498.96 Wh representing the maximum and minimum PV power generations for the specified dates respectively. The PV power generation on the other remaining days within the 7-day forecast can be forecasted in a similar way.

4.5 Economic Benefits

Solar photovoltaic module generates its energy from sunlight which is a natural source influenced by climatic conditions. The profitability of the solar PV system is therefore determined by the prevailing climatic conditions of the site location. Solar PV projects are preferred in places with a lot of sunshine.

The cost of electricity for a household tariff in Kenya is US\$ 0.217 per kWh. This includes the cost of generation, transmission, distribution and taxes. The analysis showed that for a constant daily demand of 0.44 kWh per day, with no price inflation, evaluation of equation (3.11) gives the total cost of grid electricity as US\$ 870 for the 25 years warranty period of the polycrystalline Yingli solar PV module used.

The direct cost of the solar PV system studied included the costs of PV module, battery storage system, charge controller, inverter and microcontroller. In addition, the operation and maintenance industry rates taken as 10% of investment cost \approx US\$ 28.6 from Table 3.3. For 10 years warranty period, the Yuasa lead-acid battery replaced twice. Other circuit components can operate for the 25 years project lifetime. The analysis showed that the total cost of investing in a grid tied solar PV system with a total capacity of 90 W at no subsidy to meet the load demand is evaluated by equation (3.12) using the values in Table 3.3 is US\$ 384. For the 25 years of the PV system

project lifetime, switching the connected load from the utility grid to solar PV system realized a net profit of US\$ 486.

Taking the total cost of investment as US\$ 384, energy demand as 0.44 kWh per day and unit cost of energy as US\$ 0.217 per kWh, equation (3.13) evaluated to give payback period of 11 years which is the time taken for the proposed PV system to recover itself from the initial investment cost. Beyond the 11th year, any additional saving realized from the PV system is considered as profit. This is a simple technique for appraising a project.

The PV panel efficiency decreases over time resulting to reduction in energy yield. The reduction in energy yield is referred to as 'degradation rate' and is the assumed interest rate or discount rate generally used to determine the present value of an investment. The present value of future cash flow is determined by 'discounting'. The discount rate reflects the risks involved in a project. For the 25-year warranty period of the solar PV module, the net present value is evaluated by using equation (3.14) is US\$ 119. The researcher assumed linear annual output degradation of 0.6% and a future value discount rate of 4%.

4.6 Environmental Impact

Emission intensity is defined as tons of carbon dioxide equivalent per megawatt hour (t_{CO_2}/MWh) or grams of carbon dioxide equivalent per watt-hour (g_{CO_2}/Wh), which is the lifetime carbon emission calculated per unit of energy. The environmental impact is better at lower emission intensity as less carbon dioxide emitted to produce same quantity of energy from fossil fuel.

The Energy and Petroleum Regulatory Authority (EPRA) in Kenya estimated the net grid emission factor for power plants in 2018 (still in force) at 0.3322 kgCO₂/kWh of energy generated [60]. Equation (4.1) evaluates the reduction of carbon dioxide emission by shifting production of electricity from fossil fuel to renewable energy sources [58].

$$CO_2(E_{ms}) = E_D \times 0.3322 \times 365 \times 25 \quad (4.1)$$

where $CO_2(E_{ms})$ denotes the amount of carbon dioxide emissions in kg and E_D is the energy demand in kWh per day. Equation (4.1) is evaluated and the energy management achieved through switching between PV based microgrid and the utility grid is able to reduce 1,333.78 kg of CO₂ emissions during the 25 years of the project life. The implemented prototype is still at its initial stage far from decommissioning stage where toxic substances arising from improper disposal of PV constituent materials can be considered.

4.7 Social Impact

The integration of renewable energy resource with the utility grid implemented in this study attracted many new researchers in the field. Technological advancement, community development, consumer choice and better health conditions featured with the growth in renewable energy technology.

The study faced no major challenges at start up or during its operation as regards to limitations arising from land acquisition.

CHAPTER FIVE

CONCLUSION AND FUTURE WORK

5.1 Conclusion

In this thesis, the impact of energy management in a solar PV microgrid is extensively studied. Mathematical modeling of the solar PV components following the theory of photovoltaic presented. Sizing of the PV components done considering the climatic conditions of the study site as major factors influencing the use of solar PV system in a location. The model was simulated using MATLAB/Simulink and the simulation results showed that the load was supplied from the PV module during the day; meanwhile the utility grid electricity remained as a power backup source during daytime. Additionally hardware components incorporating a microcontroller assembled for real-time implementation of the microgrid energy management. The microcontroller operated effectively by disconnecting the loads following predefined threshold limits.

The economic impact of installing a solar PV system to supplement the utility grid electricity is presented. The study concluded that the payback period for investing in a 90 W solar PV project at the study site is 11 years and the NPV estimated at \$ 119 for the 25-year warranty period of the monocrystalline PV module. This shows that a solar PV project is feasible at this site with proper design and smart operation since the weather condition of the location favors the installation of PV projects.

The study also concluded that generating electricity from solar PV system (a renewable energy source) reduces considerable quantity of CO₂ emitted into the environment when the PV module replaces the conventional grid electricity.

Historical data generated using web interface used for predicting future solar PV power generation of the installed capacity on a medium term basis. The study finally concluded that forecast weather parameters proved useful for estimating the installed PV power generation on a short-term basis. The knowledge of future power generation is beneficial to the consumer by modifying the consumer usage in both short-term and medium term basis with the assumption that the weather pattern is not adversely changing in the subsequent years around the study site.

The API software is a new technology recommended for further implementation in the field of renewable energy since it has many other parameters useful to such studies. The application is for the first time applied to estimate PV power generation in this study. No known study in literature the application used for such estimations.

5.2 Future Work of the Study

The future work of this study is to predict consumer behavior using artificial intelligence like Neuro-Fuzzy and integrate it with the energy management studied for advanced output results.

REFERENCES

- [1] A. Kirbyshire and J. Graham, "United Nations Climate Change Conferences," 11 November 2021. [Online]. Available: https://www.c40.org/what-we-do/influencing-the-global-agenda/global-diplomacy-advocacy/united-nations-climate-change-conferences-cop/?gclid=EAIaIQobChMI9PWm-tq49gIVkACLCh0cHwXAEAAAYASAAEgJybvD_BwE. [Accessed 17 November 2021].
- [2] A. G. Solanki, S. Reddy and K. Kishore, "Modeling, Simulation and Performance Analysis of Solar PV System," *International Journal for Modern Trends in Science and Technology*, vol. 7, no. 9, pp. 264-272, 2021.
- [3] M. Palmer, S. Elliott and H. Jack, "Solar Irradiance Data," Solcast, 06 February 2019. [Online]. Available: <https://solcast.com/solar-data-api/solar-irradiance-data-everywhere-you-need-it/>. [Accessed 27 July 2021].
- [4] D. Bresette, S. Bertrand and J.-M. Cross, "Environmental and Energy Study Institute," info@eesi.org, 22 July 2021. [Online]. Available: <https://www.eesi.org/topics/fossil-fuels/description>. [Accessed 23 April 2022].
- [5] info@irena.org, "International Renewable Energy Agency," IRENA, 22 June 2021. [Online]. Available: <https://www.irena.org/newsroom/pressreleases/2021/Jun/Majority-of-New->

Renewables-Undercut-Cheapest-Fossil-Fuel-on-Cost. [Accessed 16 March 2022].

- [6] K. Jäger, O. Isabella and A. H. Smets, "PV Technology," in *Solar Energy Fundamentals, Technology, and Systems*, Delft, the Netherlands, Delft University of Technology, 2014, pp. 137-141.
- [7] ©. 2.-2. R. GmbH, "ResearchGate," Electrical Impedance Spectroscopy for Photovoltaic Materials, 2022. [Online]. Available: https://www.researchgate.net/figure/The-construction-of-a-solar-cell-showing-the-different-layers-P-N-junction-and-the_fig2_348278420/download. [Accessed 02 03 2022].
- [8] C. ©. 8MSolar, "Advancing Energy Independence," 8M Solar, 2022. [Online]. Available: <https://www.8msolar.com/types-of-solar-panels>. [Accessed 08 February 2022].
- [9] Sugianto, "Comparative Analysis of Solar Cell Efficiency between Monocrystalline and Polycrystalline," *INTEK Jurnal Penelitian*, vol. 7, no. 2, pp. 92-100, 2020.
- [10] S. Senthilkumar, V. Mohan, P. Mangaiyarkarasi and M. Karthikeyan, "Analysis of Single-Diode PV Model and Optimized MPPT Model for Different Environmental Conditions," *International Transactions on Electrical Energy Systems*, vol. 2022, pp. 1-17, 2022.

- [11] G. Abdelaziz and G. Rached, "Shading effect on the performance of a photovoltaic panel," in *International Conference on Services Computing*, Tunis, 2022.
- [12] C. Okoye and U. I. Igariwey, "Solar PV Power Generation: Key Insights and Imperatives," *International Journal of Energy and Environmental Research*, vol. 7, no. 3, pp. 31-41, 2019.
- [13] J. I. Laveyne, D. Bozalakov and G. V. Eetvelde, "Impact of Solar Panel Orientation on the Integration of Solar Energy in Low-Voltage Distribution Grids," *International Journal of Photoenergy*, vol. 2020, pp. 1-13, 2020.
- [14] Y. Hamsavarthini and S. Kanthalakshmi, "Technologies In Battery Management System-A Review," *International Journal of Scientific & Technology Research*, vol. 9, no. 1, pp. 1324-1325, 2020.
- [15] J. R. Garche and K. Brandt, *Electrochemical Power Sources: Fundamentals, Systems, and Applications*, Amsterdam: Susan Dennis, 2019.
- [16] R. Zhang and S. Fujimori, "The role of transport electrification in global climate change mitigation scenarios," *Environmental Research Letters*, pp. 1-6, 19 February 2020.
- [17] P. B and K. Prof. K P Lakshmi, "Review on Battery Technology and its Challenges," *International Journal of Scientific & Engineering Research*, vol. 11, no. 09, pp. 1706-1710, 2020.
- [18] R. Keim, "Microcontroller," *All about Circuits*, p. 1, 25 March 2019.

- [19] sparkfun.com, "Electronics," SparkFun, January 2022. [Online]. Available: <https://learn.sparkfun.com/tutorials/what-is-an-arduino/all>. [Accessed 14 March 2022].
- [20] Arduino, "Arduino.cc," Arduino Week 2022 Podcast, 01 February 2022. [Online]. Available: <https://www.arduino.cc/en/Guide/Introduction>. [Accessed 04 May 2022].
- [21] tutorialspoint.com, "Arduino - Board Description," Tutorials Point India Private Limited, 2022. [Online]. Available: https://www.tutorialspoint.com/arduino/arduino_board_description.htm. [Accessed 16 May 2022].
- [22] amazon.co.uk, "Arduino Uno REV3," Amazon, 18 May 2022. [Online]. Available: https://www.amazon.co.uk/Arduino-A000066-ARDUINO-UNO-REV3/dp/B008GRTSV6/ref=sr_1_1?crid=38YV9ZT6DAF1D&keywords=ARDUINO+A000066+Uno+R3&qid=1652879764&sprefix=arduino+a000066+uno+r3%2Caps%2C560&sr=8-1. [Accessed 18 May 2022].
- [23] N. J. Imu, A. Ezeamama and S. Matemilola, "Assessment of energy and emissions saving impact of solar PV modules," *International Journal of Building Pathology and Adaptation*, pp. 1-14, 2021.
- [24] energysavingtrust.org.uk, "Solar panels," Energy Saving Trust, 06 May 2022. [Online]. Available: <https://energysavingtrust.org.uk/advice/solar-panels/>. [Accessed 14 May 2022].
- [25] S. A. Robinson and G. A. Meindl, "Potential for leaching of heavy metals and metalloids from crystalline silicon photovoltaic systems," *Journal of Natural Resources and Development*, vol. 09, pp. 19-24, 2019.

- [26] A. Gawande and P. Chaudhry, "Environmental and Social Impacts of Solar Energy," *Jharkhand Journal of Development and Management Studies*, vol. 17, no. 2, pp. 8115-8125, 2019.
- [27] I. R. E. Agency, "International Renewable Energy Agency," 2022. [Online]. Available: <https://www.irena.org/solar>. [Accessed 03 January 2022].
- [28] A. Hota, S. K. Bhuyan and P. K. Hota, "Modeling & Simulation of Photovoltaic System Connected to Grid using Matlab," in *ICREISG*, Bhubaneswar, 2020.
- [29] D. Chippada and D. Reddy, "Mathematical modeling and simulation of energy management in smart grid," *International Journal of Smart Grid and Clean Energy*, vol. 9, no. 4, pp. 746-755, 2020.
- [30] Muhardika and Syafii, "Design of arduino-based loading management system to improve continuity of solar power supply," *Indonesian Journal of Electrical Engineering and Computer Science*, vol. 20, no. 3, pp. 1677-1684, 2020.
- [31] A. Mujahid and M. S. Rehman, "Power-saving smart energy grid meter for blackout management," *Journal of Applied Science and Engineering*, vol. 24, no. 4, pp. 491-498, 2021.
- [32] K. C. Meje, L. Bokopane and K. Kusakana, "Real-time power dispatch in a standalone hybrid multisource distributed energy system using an Arduino board," Elsevier Ltd., Bloemfontein, South Africa, 2021.

- [33] Q. A. Alabdali and A. M. Nahhas, "Simulation Study of Grid Connected Photovoltaic System Using PVsyst Software: Analytical Study for Yanbu and Rabigh Regions in Saudi Arabia," *American Journal of Energy Research*, vol. 9, no. 1, pp. 30-44, 2021.
- [34] F. H. Faiz, R. Shakoor and A. Raheem, "Modeling and Analysis of 3MW Solar Photovoltaic Plant Using PVSyst at Islamia University of Bahawalpur, Pakistan," *International Journal of Photoenergy, Hindawi*, vol. 2021, pp. 1-14, 2021.
- [35] M. H. Chung, "Estimating Solar Insolation and Power Generation of Photovoltaic Systems Using Previous Day Weather Data," *Advances in Civil Engineering*, vol. 2020, pp. 1-12, 18 February 2020.
- [36] J. M. Bright, "Solcast: Validation of a satellite-derived solar irradiance dataset," *Solar Energy*, pp. 1-22, 04 August 2019.
- [37] H. Al-Zoubi, Y. Al-Khasawneh and W. Omar, "Design and feasibility study of an on-grid photovoltaic system for green electrification of hotels: a case study of Cedars hotel," *International Journal of Energy and Environmental Engineering*, vol. 10, pp. 616-626, 2021.
- [38] P. Thanarak and K. Lhazom, "Economic Feasibility Analysis of Off-Grid PV Systems for Remote Settlements in Bhutan," *International Journal of Energy Economics and Policy*, vol. 11, no. 3, pp. 206-214, 2021.
- [39] Z. Šimić, D. Topić and I. Crnogorac, "Method for Sizing of a PV System for Family Home Using Economic Indicators," *energies*, pp. 1-18, 27 July 2021.
- [40] EPA, "epa.gov/ghgemissions/overview-greenhouse-gase," United States Environmental Protection Agency, 19 November 2021. [Online]. Available:

<https://www.epa.gov/ghgemissions/overview-greenhouse-gases>. [Accessed 17 March 2022].

- [41] A. Edianto, G. Trencher and K. Matsubae, "Why do some countries receive more international financing for," *Energy for Sustainable Development*, vol. 12, no. 004, pp. 177-188, 2022.
- [42] M. Motyka, K. Hardin and J. Thomson, "Deloitte Resources 2020 Study," Deloitte, 2020. [Online]. Available: <https://www2.deloitte.com/us/en/insights/industry/power-and-utilities/energy-study-of-businesses-and-residential-consumers.html>. [Accessed 21 April 2022].
- [43] S. Bagal, J. Dhobale, A. Sarve and R. Satone, "Arduino Based Automatic Plant Watering System," *International Journal of Engineering Science and Computing*, vol. 8, no. 3, pp. 1-3, 2018.
- [44] A. D. Dhass, N. Beemkumar, S. Harikrishnan and H. M. Ali, "A Review on Factors Influencing the Mismatch Losses in Solar PV System," *International Journal of Photoenergy*, vol. 2022, pp. 3-16, 2022.
- [45] S. Senthilkumar, V. Mohan and P. Mangaiyarkarasi, "Analysis of Single-Diode PV Model and Optimized MPPT Model for Different Environmental Conditions," *International Transactions on Electrical Energy Systems*, pp. 3-5, 31 January 2022.
- [46] M. Azaroual, M. Ouassaid and M. Maaroufi, "Optimum Energy Flow Management of a Grid-Tied PV-Wind-Battery System considering Cost, Reliability, and CO₂ Emission," *International Journal of Photoenergy, Hindawi*, vol. 2021, pp. 1-20, 2021.

- [47] A. Bakundukize, M. Twizerimana and D. Bernadette, "Design and Modelling of PV Power Plant for Rural Electrification in Kayonza, Rwanda," *Journal of Energy Research and Reviews*, vol. 7, no. 4, pp. 31-55, 2021.
- [48] S. Jiang and Z. Song, "A review on the state of health estimation methods of lead-acid batteries," *Journal of Power Sources*, vol. 10, pp. 1-18, 2021.
- [49] A. Bakundukize, M. Twizerimana and D. Bernadette, "Design and Modelling of PV Power Plant for Rural Electrification in Kayonza, Rwanda," *Journal of Energy Research and Reviews*, vol. 7, no. 4, pp. 31-55, 2021.
- [50] jan@weather-and-climate.com, "weather-and-climate.com," 2010-2022 World Weather & Climate Information, 2022. [Online]. Available: <https://weather-and-climate.com/average-monthly-hours-Sunshine,muranga-ke,Kenya>. [Accessed 03 January 2022].
- [51] B. Aboagye, S. Gyamfi, J. C. Puoza and M. Obeng, "Techno-economic Feasibility Analysis of Solar Photovoltaic System for Single Households in Peri-urban Areas Kumasi, Ghana," *International Journal of Sustainable Energy Development*, vol. 8, no. 1, pp. 392-404, 2020.
- [52] J. Gumpf and R. Lachika, "Solar Stik," solarstik.com, 2022. [Online]. Available: <https://solarstik.com/stikopedia/calculate-inverter-size/>. [Accessed 25 October 2022].
- [53] A. Mahmood, "Design and Simulation of Stand-alone PV System for Electronic and Communications Engineering Department Laboratories in Al-Nahrain University," *EAI Endorsed Transactions on*, vol. 6, no. 21, pp. 1-6, 2019.

- [54] Jumia, "Brands and categories," June 2022. [Online]. Available: <https://www.jumia.co.ke/catalog/?q=solar+panel+fullkit>. [Accessed 13 June 2022].
- [55] Ghrzuzudu, "Myloview," 2022. [Online]. Available: <https://myloview.de/bild-high-voltage-power-line-transmission-tower-or-electricity-pylon-nr-971BAC8>.
- [56] dmca@coursehero.com., "Earth Science," The CliffsNotes website, 2022. [Online]. Available: <https://www.cliffsnotes.com/study-guides/earth-science/insolation-and-seasons-on-earth/solar-radiation>. [Accessed 16 April 2022].
- [57] Z. Šimić, D. Topić and I. Crnogorac, "Method for Sizing of a PV System for Family Home Using Economic Indicators," *MDPI*, vol. 14, no. 4529, pp. 1-18, 2021.
- [58] C. A. Hossain, N. Chowdhury and M. Longo, "System and Cost Analysis of Stand-Alone Solar Home System Applied to a Developing Country," *MDPI*, vol. 11, no. 1403, pp. 1-13, 2019.
- [59] F. Obeidat and I. Rahoma, "One Year Real Data Rooftop PV System Performance Analysis of a University Academic Campus," *International Journal on Energy Conversion*, vol. 9, no. 4, pp. 168-174, 2021.
- [60] P. R. Oimeke, "Energy & Petroleum Statistics Report 2019," EPRA Publication 2019, Nairobi, 2019.

APPENDICES

APPENDIX A: YINGLI 90 W ELECTRICAL CHARACTERISTICS

5/3/22, 5:22 PM

Print version

Yingli 80W/85W/90W Polycrystalline Solar Module



ELECTRICAL PERFORMANCE

Electrical parameters at Standard Test Conditions (STC)

Module name	YGE 90	YGE 85	YGE 80
Module type	YL090P-17b 2/3	YL085P-17b 2/3	YL080P-17b 2/3
Power output Pmax W	90	85	80
Power output tolerances ΔPmax %		+/- 3	
Module efficiency ηm %	13.5	12.8	12.0
Voltage at Pmax Vmpp V	17.5	17.5	17.0
Current at Pmax Impp A	5.14	4.86	4.71
Open-circuit voltage Voc V	22.0	22.0	22.0
Short-circuit current Isc A	5.60	5.36	5.04

Electrical parameters at Nominal Operating Cell Temperature (NOCT)

Power output Pmax W	65.4	65.4	58.1
Voltage at Pmax Vmpp V	16.0	16.0	15.5
Current at Pmax Impp A	4.09	4.09	3.75
Open-circuit voltage Voc V	20.1	20.1	20.1
Short-circuit current Isc A	4.54	4.54	4.54

STC: 1000W/m² irradiance, 25°C T_{module}, AM 1.5g spectrum according to EN 60904-3. Ave. efficiency reduction of 5% at 200W/m² according to EN 60904-1.
 NOCT: open-circuit module operation temperature at 800W/m² irradiance, 20°C T_{ambient}, 1m/s wind speed.

<https://www.jpcosolar.com/products/yingli-12v-solar-panel/80w-85w-90w/?print=1>

1/2

APPENDIX B: YUASA TECHNICAL DATA SHEET

Yuasa Technical Data Sheet

Yuasa NP65-12I Industrial VRLA Battery

Specifications	
Nominal voltage (V)	12
20-hr rate Capacity to 10.5V at 20°C (Ah)	65
10-hr rate Capacity to 10.8V at 20°C (Ah)	60.5
Dimensions	
Length (mm)	350 (±1)
Width (mm)	166 (±1)
Height (mm)	174 (±2)
Mass (kg)	23
Terminal Type	
Threaded terminal - (M=Male or F=Female)	M6 (F)
Torque (Nm)	4.76
Operating Temperature Range	
Storage (in fully charged condition)	-20°C to +60°C
Charge	-15°C to +50°C
Discharge	-20°C to +60°C
Storage	
Capacity loss per month at 20°C (% approx.)	3
Case Material	
Standard	ABS (UL94:HB)
Charge Voltage	
Float charge voltage at 20°C (V)/Block	13.65 (±1%)
Float charge voltage at 20°C (V)/Cell	2.275 (±1%)
Float Chg voltage tmp correction factor from std 20°C (mV)	-3
Cyclic (or Boost) charge Voltage at 20°C (V)/Block	14.5 (±3%)
Cyclic (or Boost) charge Voltage at 20°C (V)/Cell	2.42 (±3%)
Cyclic Chg voltage tmp correction factor from std 20°C (mV)	-4
Charge Current	
Float charge current limit (A)	No limit
Cyclic (or Boost) charge current limit (A)	16.25
Maximum Discharge Current	
1 second (A)	800
1 minute (A)	500
Short-Circuit Current & Internal Resistance	
Internal resistance - according to EN IEC 60896-21 (mΩ)	10.51
Short-Circuit current - according to EN IEC 60896-21 (A)	1375
Impedance	
Measured at 1 kHz (mΩ)	7
Design Life & Approvals	
EUROBAT Classification: Standard Commercial	3 to 5
Yuasa design life at 20°C (yrs)	up to 5
VdS (Germany)	VdS No: G 183008



Layout



3rd Party Certifications

ISO9001 - Quality Management Systems
 ISO14001 - Environmental Management Systems
 EN 18001 OHSAS Management Systems
 UNDERWRITERS LABORATORIES Inc.



Safety

Installation

Can be installed and operated in any orientation except permanently inverted.

Handles

Batteries must not be suspended by their handles (where fitted).

Vent valves

Each cell is fitted with a low pressure release valve to allow gasses to escape and then reseal.

Gas release

VRLA batteries release hydrogen gas which can form explosive mixtures in the air. Do not place inside a sealed container.

Recycling

YUASA's VRLA batteries must be recycled at the end of life in accordance with local and national laws and regulations.

Data Sheet generated on 05/11/2019 - E&OE



The world's leading battery manufacturer

www.yuasaeurope.com



APPENDIX C: MATLAB CODE FOR PV SYSTEM MODELING

```
---- Sorted list for 'power_HEMS' [599 nonvirtual block(s), directFeed=0]
0:0 'power_HEMS/powergui/EquivalentModel1/Sources/SwitchCurrents' (Constant, tid=PRM)
0:1 'power_HEMS/Battery/Battery/Model/Constant1' (Constant, tid=PRM)
0:2 'power_HEMS/Battery/Battery/Model/Constant' (Constant, tid=PRM)
0:3 'power_HEMS/Battery/Battery/Model/it init1' (Memory, tid=1)
0:4 'power_HEMS/Battery/Battery/Model/R2' (Gain, tid=1)
0:5 'power_HEMS/Battery/Battery/Model/Fcn9' (Fcn, tid=1)
0:6 'power_HEMS/Battery/Battery/Model/Current filter' (DiscreteTransferFcn, tid=2)
0:7 'power_HEMS/Battery/Battery/Model/Compare To Zero/Constant' (Constant, tid=CONSTANT)
0:8 'power_HEMS/Battery/Battery/Model/Compare To Zero/Compare' (RelationalOperator, tid=2)
0:9 'power_HEMS/Battery/Battery/Model/Data Type Conversion2' (DataTypeConversion, tid=2)
0:10 'power_HEMS/Battery/Battery/Model/it init' (Memory, tid=1)
0:11 'power_HEMS/Battery/Battery/Model/int(i)' (DiscreteIntegrator, tid=2)
0:12 'power_HEMS/Battery/Battery/Model/Gain' (Gain, tid=2)
0:13 'power_HEMS/Battery/Battery/Model/Saturation Dynamic1/LowerRelop1' (RelationalOperator, tid=1)
0:14 'power_HEMS/Battery/Battery/Model/Constant9' (Constant, tid=PRM)
0:15 'power_HEMS/Battery/Battery/Model/Saturation Dynamic1/UpperRelop' (RelationalOperator, tid=2)
0:16 'power_HEMS/Battery/Battery/Model/Saturation Dynamic1/Switch' (Switch, tid=2)
0:17 'power_HEMS/Battery/Battery/Model/Saturation Dynamic1/Switch2' (Switch, tid=1)
0:18 'power_HEMS/Battery/Battery/Model/Relational Operator' (RelationalOperator, tid=1)
0:19 'power_HEMS/Battery/Battery/Model/Switch7' (Switch, tid=1)
0:20 'power_HEMS/Battery/Battery/Model/E_NL' (Fcn, tid=1)
0:21 'power_HEMS/Battery/Battery/Model/E_dyn Discharge' (Fcn, tid=1)
0:22 'power_HEMS/Battery/Battery/Model/E_dyn Charge/Constant' (Constant, tid=PRM)
0:23 'power_HEMS/Battery/Battery/Model/E_dyn Charge/Constant4' (Constant, tid=PRM)
0:24 'power_HEMS/Battery/Battery/Model/R3' (Gain, tid=1)
0:25 'power_HEMS/Battery/Battery/Model/Saturation Dynamic2/LowerRelop1' (RelationalOperator, tid=1)
0:26 'power_HEMS/Battery/Battery/Model/Fcn6' (Fcn, tid=1)
0:27 'power_HEMS/Battery/Battery/Model/Saturation Dynamic2/UpperRelop' (RelationalOperator, tid=1)
0:28 'power_HEMS/Battery/Battery/Model/Saturation Dynamic2/Switch' (Switch, tid=1)
```

APPENDIX D1: ARDUINO UNO TECHNICAL SPECIFICATIONS

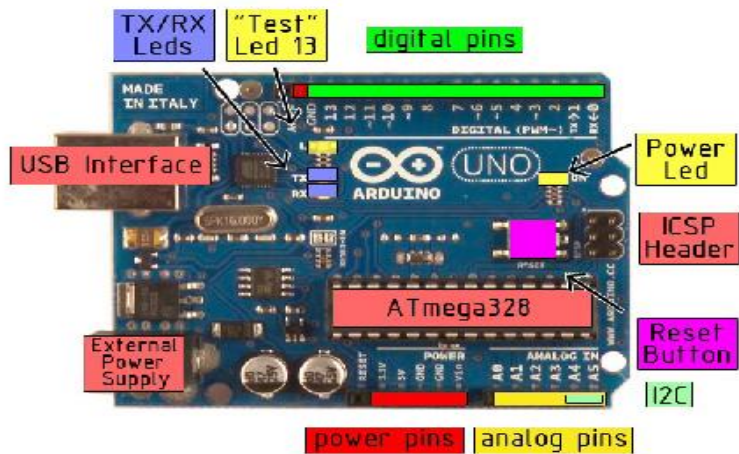
Technical Specification

EAGLE files: [arduino-duemilanove-uno-design.zip](#) Schematic: [arduino-uno-schematic.pdf](#)

Summary

Microcontroller	ATmega328
Operating Voltage	5V
Input Voltage (recommended)	7-12V
Input Voltage (limits)	6-20V
Digital I/O Pins	14 (of which 6 provide PWM output)
Analog Input Pins	6
DC Current per I/O Pin	40 mA
DC Current for 3.3V Pin	50 mA
Flash Memory	32 KB of which 0.5 KB used by bootloader
SRAM	2 KB
EEPROM	1 KB
Clock Speed	16 MHz

the board



APPENDIX D2: ARDUINO UNO TECHNICAL SPECIFICATIONS

Power

The Arduino Uno can be powered via the USB connection or with an external power supply. The power source is selected automatically.

External (non-USB) power can come either from an AC-to-DC adapter (wall-wart) or battery. The adapter can be connected by plugging a 2.1mm center-positive plug into the board's power jack. Leads from a battery can be inserted in the Gnd and Vin pin headers of the POWER connector.

The board can operate on an external supply of 6 to 20 volts. If supplied with less than 7V, however, the 5V pin may supply less than five volts and the board may be unstable. If using more than 12V, the voltage regulator may overheat and damage the board. The recommended range is 7 to 12 volts.

The power pins are as follows:

- **VIN.** The input voltage to the Arduino board when it's using an external power source (as opposed to 5 volts from the USB connection or other regulated power source). You can supply voltage through this pin, or, if supplying voltage via the power jack, access it through this pin.
- **5V.** The regulated power supply used to power the microcontroller and other components on the board. This can come either from VIN via an on-board regulator, or be supplied by USB or another regulated 5V supply.
- **3V3.** A 3.3 volt supply generated by the on-board regulator. Maximum current draw is 50 mA.
- **GND.** Ground pins.

Memory

The Atmega328 has 32 KB of flash memory for storing code (of which 0,5 KB is used for the bootloader); It has also 2 KB of SRAM and 1 KB of EEPROM (which can be read and written with the [EEPROM library](#)).

Input and Output

Each of the 14 digital pins on the Uno can be used as an input or output, using [pinMode\(\)](#), [digitalWrite\(\)](#), and [digitalRead\(\)](#) functions. They operate at 5 volts. Each pin can provide or receive a maximum of 40 mA and has an internal pull-up resistor (disconnected by default) of 20-50 kOhms. In addition, some pins have specialized functions:

- **Serial: 0 (RX) and 1 (TX).** Used to receive (RX) and transmit (TX) TTL serial data. These pins are connected to the corresponding pins of the ATmega8U2 USB-to-TTL Serial chip.
- **External Interrupts: 2 and 3.** These pins can be configured to trigger an interrupt on a low value, a rising or falling edge, or a change in value. See the [attachInterrupt\(\)](#) function for details.
- **PWM: 3, 5, 6, 9, 10, and 11.** Provide 8-bit PWM output with the [analogWrite\(\)](#) function.
- **SPI: 10 (SS), 11 (MOSI), 12 (MISO), 13 (SCK).** These pins support SPI communication, which, although provided by the underlying hardware, is not currently included in the Arduino language.
- **LED: 13.** There is a built-in LED connected to digital pin 13. When the pin is HIGH value, the LED is on, when the pin is LOW, it's off.



radiospares

RADIONICS



APPENDIX D3: ARDUINO CODE FOR PROGRAM INITIALIZATION

```
/*ENERGY MANAGEMENT SYSTEM*/
#include <OneWire.h>
#include <LiquidCrystal_I2C.h>
LiquidCrystal_I2C lcd(0x27, 16, 2);
//RELAYS TO CONTROL LOAD ONE
int solarlive1=2;
int solarneutra1=3;
int gridlive11=8;
int gridneutra11=9;
//RELAYS TO CONTROL LOAD TWO
int solarlive2=4;
int solarneutra2=5;
int gridlive22=10;
int gridneutra22=11;
//RELAYS TO CONTROL LOAD THREE
int solarlive3=6;
int solarneutra3=7;
int gridlive33=12;
int gridneutra33=13;
const int sensorIn = A0;
int mVperAmp = 185;
double Voltage = 0;
double VRMS = 0;
double AmpsRMS = 0;
double current=0;
void setup(){
  lcd.begin();
  Serial.begin(9600);
  pinMode(solarlive1 ,OUTPUT);
  pinMode( solarneutra1 ,OUTPUT);
```

APPENDIX E: ACS712 CURRENT SENSOR DATASHEET

ACS712

Fully Integrated, Hall-Effect-Based Linear Current Sensor IC
with 2.1 kVRMS Isolation and a Low-Resistance Current Conductor

x05B PERFORMANCE CHARACTERISTICS [1]: $T_A = -40^{\circ}\text{C}$ to 85°C , $C_F = 1\text{ nF}$, and $V_{CC} = 5\text{ V}$, unless otherwise specified

Characteristic	Symbol	Test Conditions	Min.	Typ.	Max.	Units
Optimized Accuracy Range	I_p		-5	-	5	A
Sensitivity	Sens	Over full range of I_p , $T_A = 25^{\circ}\text{C}$	180	185	190	mV/A
Noise	$V_{\text{NOISE(PP)}}$	Peak-to-peak, $T_A = 25^{\circ}\text{C}$, 185 mV/A programmed Sensitivity, $C_F = 47\text{ nF}$, $C_{\text{OUT}} = \text{open}$, 2 kHz bandwidth	-	21	-	mV
Zero Current Output Slope	$\Delta V_{\text{OUT(0)}}$	$T_A = -40^{\circ}\text{C}$ to 25°C	-	-0.26	-	mV/°C
		$T_A = 25^{\circ}\text{C}$ to 150°C	-	-0.08	-	mV/°C
Sensitivity Slope	ΔSens	$T_A = -40^{\circ}\text{C}$ to 25°C	-	0.054	-	mV/A/°C
		$T_A = 25^{\circ}\text{C}$ to 150°C	-	-0.008	-	mV/A/°C
Total Output Error [2]	E_{TOT}	$I_p = \pm 5\text{ A}$, $T_A = 25^{\circ}\text{C}$	-	± 1.5	-	%

[1] Device may be operated at higher primary current levels, I_p , and ambient temperatures, T_A , provided that the Maximum Junction Temperature, $T_{j(\text{max})}$, is not exceeded.

[2] Percentage of I_p , with $I_p = 5\text{ A}$. Output filtered.

x20A PERFORMANCE CHARACTERISTICS [1]: $T_A = -40^{\circ}\text{C}$ to 85°C , $C_F = 1\text{ nF}$, and $V_{CC} = 5\text{ V}$, unless otherwise specified

Characteristic	Symbol	Test Conditions	Min.	Typ.	Max.	Units
Optimized Accuracy Range	I_p		-20	-	20	A
Sensitivity	Sens	Over full range of I_p , $T_A = 25^{\circ}\text{C}$	96	100	104	mV/A
Noise	$V_{\text{NOISE(PP)}}$	Peak-to-peak, $T_A = 25^{\circ}\text{C}$, 100 mV/A programmed Sensitivity, $C_F = 47\text{ nF}$, $C_{\text{OUT}} = \text{open}$, 2 kHz bandwidth	-	11	-	mV
Zero Current Output Slope	$\Delta V_{\text{OUT(0)}}$	$T_A = -40^{\circ}\text{C}$ to 25°C	-	-0.34	-	mV/°C
		$T_A = 25^{\circ}\text{C}$ to 150°C	-	-0.07	-	mV/°C
Sensitivity Slope	ΔSens	$T_A = -40^{\circ}\text{C}$ to 25°C	-	0.017	-	mV/A/°C
		$T_A = 25^{\circ}\text{C}$ to 150°C	-	-0.004	-	mV/A/°C
Total Output Error [2]	E_{TOT}	$I_p = \pm 20\text{ A}$, $T_A = 25^{\circ}\text{C}$	-	± 1.5	-	%

[1] Device may be operated at higher primary current levels, I_p , and ambient temperatures, T_A , provided that the Maximum Junction Temperature, $T_{j(\text{max})}$, is not exceeded.

[2] Percentage of I_p , with $I_p = 20\text{ A}$. Output filtered.

x30A PERFORMANCE CHARACTERISTICS [1]: $T_A = -40^{\circ}\text{C}$ to 85°C , $C_F = 1\text{ nF}$, and $V_{CC} = 5\text{ V}$, unless otherwise specified

Characteristic	Symbol	Test Conditions	Min.	Typ.	Max.	Units
Optimized Accuracy Range	I_p		-30	-	30	A
Sensitivity	Sens	Over full range of I_p , $T_A = 25^{\circ}\text{C}$	63	66	69	mV/A
Noise	$V_{\text{NOISE(PP)}}$	Peak-to-peak, $T_A = 25^{\circ}\text{C}$, 66 mV/A programmed Sensitivity, $C_F = 47\text{ nF}$, $C_{\text{OUT}} = \text{open}$, 2 kHz bandwidth	-	7	-	mV
Zero Current Output Slope	$\Delta V_{\text{OUT(0)}}$	$T_A = -40^{\circ}\text{C}$ to 25°C	-	-0.35	-	mV/°C
		$T_A = 25^{\circ}\text{C}$ to 150°C	-	-0.08	-	mV/°C
Sensitivity Slope	ΔSens	$T_A = -40^{\circ}\text{C}$ to 25°C	-	0.007	-	mV/A/°C
		$T_A = 25^{\circ}\text{C}$ to 150°C	-	-0.002	-	mV/A/°C
Total Output Error [2]	E_{TOT}	$I_p = \pm 30\text{ A}$, $T_A = 25^{\circ}\text{C}$	-	± 1.5	-	%

[1] Device may be operated at higher primary current levels, I_p , and ambient temperatures, T_A , provided that the Maximum Junction Temperature, $T_{j(\text{max})}$, is not exceeded.

[2] Percentage of I_p , with $I_p = 30\text{ A}$. Output filtered.



Allegro MicroSystems
955 Perimeter Road
Manchester, NH 03103-3353 U.S.A.
www.allegromicro.com

5

APPENDIX F1: API FORECAST 12TH MARCH 2022

Ghi	Ghi90	Ghi10	Ebh	Dni	Dni10	Dni90	Dhi	air_temp	Zenith	Azimuth	cloud_op	period_end	Period
963	963	915	839	961	913	961	125	27	30	-97	0	2022-03-11T08:00:00Z	PT30M
1033	1033	982	905	976	928	976	129	28	22	-99	0	2022-03-11T08:30:00Z	PT30M
1084	1084	1029	950	984	934	984	134	28	15	-104	0	2022-03-11T09:00:00Z	PT30M
1113	1113	1031	975	986	830	986	139	28	8	-117	0	2022-03-11T09:30:00Z	PT30M
1116	1121	901	967	971	445	982	149	29	4	171	0	2022-03-11T10:00:00Z	PT30M
1105	1108	805	963	976	273	985	142	29	9	114	0	2022-03-11T10:30:00Z	PT30M
1071	1072	724	936	975	183	979	134	30	16	103	0	2022-03-11T11:00:00Z	PT30M
1024	1024	635	902	979	122	979	122	30	23	99	0	2022-03-11T11:30:00Z	PT30M
947	947	596	838	977	134	977	110	30	31	97	0	2022-03-11T12:00:00Z	PT30M
855	855	522	748	949	113	949	107	30	38	96	0	2022-03-11T12:30:00Z	PT30M
730	744	417	618	889	73	921	112	29	46	95	1	2022-03-11T13:00:00Z	PT30M
610	622	323	500	830	50	874	110	29	53	95	1	2022-03-11T13:30:00Z	PT30M
479	489	239	387	798	37	810	93	28	61	94	2	2022-03-11T14:00:00Z	PT30M
340	350	164	246	656	28	717	94	28	68	94	2	2022-03-11T14:30:00Z	PT30M
200	210	93	126	522	21	573	74	27	76	94	4	2022-03-11T15:00:00Z	PT30M
73	81	33	26	156	9	218	47	25	83	94	8	2022-03-11T15:30:00Z	PT30M
0	0	0	0	0	0	0	0	23	90	94	16	2022-03-11T16:00:00Z	PT30M
0	0	0	0	0	0	0	0	21	98	94	15	2022-03-11T16:30:00Z	PT30M
0	0	0	0	0	0	0	0	19	105	94	6	2022-03-11T17:00:00Z	PT30M
0	0	0	0	0	0	0	0	18	113	95	1	2022-03-11T17:30:00Z	PT30M
0	0	0	0	0	0	0	0	17	120	95	1	2022-03-11T18:00:00Z	PT30M
0	0	0	0	0	0	0	0	17	128	96	1	2022-03-11T18:30:00Z	PT30M
0	0	0	0	0	0	0	0	17	135	97	1	2022-03-11T19:00:00Z	PT30M
0	0	0	0	0	0	0	0	17	143	98	1	2022-03-11T19:30:00Z	PT30M
0	0	0	0	0	0	0	0	17	150	100	0	2022-03-11T20:00:00Z	PT30M
0	0	0	0	0	0	0	0	16	158	103	0	2022-03-11T20:30:00Z	PT30M
0	0	0	0	0	0	0	0	16	165	109	0	2022-03-11T21:00:00Z	PT30M
0	0	0	0	0	0	0	0	16	172	125	0	2022-03-11T21:30:00Z	PT30M
0	0	0	0	0	0	0	0	16	175	-174	0	2022-03-11T22:00:00Z	PT30M
0	0	0	0	0	0	0	0	16	171	-121	0	2022-03-11T22:30:00Z	PT30M
0	0	0	0	0	0	0	0	14	164	-107	0	2022-03-11T23:00:00Z	PT30M
0	0	0	0	0	0	0	0	14	156	-102	0	2022-03-11T23:30:00Z	PT30M
0	0	0	0	0	0	0	0	14	149	-99	0	3/12/2022	PT30M
0	0	0	0	0	0	0	0	14	142	-97	0	2022-03-12T00:30:00Z	PT30M
0	0	0	0	0	0	0	0	14	134	-96	0	2022-03-12T01:00:00Z	PT30M
0	0	0	0	0	0	0	0	14	127	-96	0	2022-03-12T01:30:00Z	PT30M
0	0	0	0	0	0	0	0	14	119	-95	0	2022-03-12T02:00:00Z	PT30M
0	0	0	0	0	0	0	0	14	112	-95	0	2022-03-12T02:30:00Z	PT30M
0	0	0	0	0	0	0	0	14	104	-94	0	2022-03-12T03:00:00Z	PT30M
0	0	0	0	0	0	0	0	14	97	-94	0	2022-03-12T03:30:00Z	PT30M
4	4	2	1	6	0	6	3	14	89	-94	0	2022-03-12T04:00:00Z	PT30M
103	103	45	51	299	12	299	52	17	82	-94	0	2022-03-12T04:30:00Z	PT30M
237	237	110	155	561	19	561	83	19	74	-94	0	2022-03-12T05:00:00Z	PT30M
380	380	190	296	758	32	758	85	21	67	-94	0	2022-03-12T05:30:00Z	PT30M
521	521	274	421	816	45	816	100	22	59	-94	0	2022-03-12T06:00:00Z	PT30M
654	654	364	556	903	66	903	98	23	52	-94	0	2022-03-12T06:30:00Z	PT30M
775	775	472	664	924	103	924	110	24	44	-95	0	2022-03-12T07:00:00Z	PT30M
880	880	563	770	965	139	965	110	25	37	-95	0	2022-03-12T07:30:00Z	PT30M
971	971	630	858	991	156	991	112	27	30	-97	0	2022-03-12T08:00:00Z	PT30M
1042	1042	676	918	989	153	989	123	27	22	-98	0	2022-03-12T08:30:00Z	PT30M

APPENDIX F2: API FORECAST 13TH MARCH 2022

Ghi	Ghi90	Ghi10	Ebh	Dni	Dni10	Dni90	Dhi	air_temp	Zenith	Azimuth	cloud_op	period_end	Period
1092	1092	700	965	999	142	999	128	28	15	-102	0	2022-03-12T09:00:00Z	PT30M
1121	1121	706	987	997	126	997	134	28	8	-114	0	2022-03-12T09:30:00Z	PT30M
1129	1129	711	987	988	123	988	142	29	3	169	0	2022-03-12T10:00:00Z	PT30M
1116	1116	703	983	994	128	994	133	29	9	111	0	2022-03-12T10:30:00Z	PT30M
1079	1079	690	952	991	143	991	126	30	16	101	0	2022-03-12T11:00:00Z	PT30M
1024	1024	675	902	979	168	979	122	30	23	98	0	2022-03-12T11:30:00Z	PT30M
940	949	607	820	957	147	977	119	30	31	96	1	2022-03-12T12:00:00Z	PT30M
829	855	518	691	877	109	949	138	30	38	95	2	2022-03-12T12:30:00Z	PT30M
694	744	400	535	770	60	919	159	29	46	95	6	2022-03-12T13:00:00Z	PT30M
564	622	297	392	652	34	873	172	29	53	94	9	2022-03-12T13:30:00Z	PT30M
441	488	218	296	611	25	811	144	28	61	94	9	2022-03-12T14:00:00Z	PT30M
316	350	145	189	505	17	718	126	28	68	94	9	2022-03-12T14:30:00Z	PT30M
183	210	81	89	368	12	577	94	27	76	94	12	2022-03-12T15:00:00Z	PT30M
61	81	25	12	73	6	218	49	25	83	94	23	2022-03-12T15:30:00Z	PT30M
0	0	0	0	0	0	0	0	23	91	94	42	2022-03-12T16:00:00Z	PT30M
0	0	0	0	0	0	0	0	21	98	94	50	2022-03-12T16:30:00Z	PT30M
0	0	0	0	0	0	0	0	19	106	94	49	2022-03-12T17:00:00Z	PT30M
0	0	0	0	0	0	0	0	18	113	94	48	2022-03-12T17:30:00Z	PT30M
0	0	0	0	0	0	0	0	17	120	95	45	2022-03-12T18:00:00Z	PT30M
0	0	0	0	0	0	0	0	17	128	95	42	2022-03-12T18:30:00Z	PT30M
0	0	0	0	0	0	0	0	17	135	96	40	2022-03-12T19:00:00Z	PT30M
0	0	0	0	0	0	0	0	17	143	97	38	2022-03-12T19:30:00Z	PT30M
0	0	0	0	0	0	0	0	16	150	99	37	2022-03-12T20:00:00Z	PT30M
0	0	0	0	0	0	0	0	16	158	102	34	2022-03-12T20:30:00Z	PT30M
0	0	0	0	0	0	0	0	16	165	107	29	2022-03-12T21:00:00Z	PT30M
0	0	0	0	0	0	0	0	16	172	123	25	2022-03-12T21:30:00Z	PT30M
0	0	0	0	0	0	0	0	14	176	-172	21	2022-03-12T22:00:00Z	PT30M
0	0	0	0	0	0	0	0	14	171	-119	14	2022-03-12T22:30:00Z	PT30M
0	0	0	0	0	0	0	0	14	164	-106	5	2022-03-12T23:00:00Z	PT30M
0	0	0	0	0	0	0	0	14	156	-101	0	2022-03-12T23:30:00Z	PT30M
0	0	0	0	0	0	0	0	14	149	-98	0	3/13/2022	PT30M
0	0	0	0	0	0	0	0	14	142	-97	0	2022-03-13T00:00:00Z	PT30M
0	0	0	0	0	0	0	0	14	134	-96	0	2022-03-13T01:00:00Z	PT30M
0	0	0	0	0	0	0	0	14	127	-95	0	2022-03-13T01:30:00Z	PT30M
0	0	0	0	0	0	0	0	13	119	-95	0	2022-03-13T02:00:00Z	PT30M
0	0	0	0	0	0	0	0	13	112	-94	0	2022-03-13T02:30:00Z	PT30M
0	0	0	0	0	0	0	0	13	104	-94	0	2022-03-13T03:00:00Z	PT30M
0	0	0	0	0	0	0	0	13	97	-94	0	2022-03-13T03:30:00Z	PT30M
4	4	3	1	6	0	6	4	14	89	-94	0	2022-03-13T04:00:00Z	PT30M
102	102	65	50	294	41	294	52	16	82	-93	0	2022-03-13T04:30:00Z	PT30M
236	236	156	152	551	91	551	84	19	74	-93	0	2022-03-13T05:00:00Z	PT30M
379	379	262	293	737	154	737	86	21	67	-94	0	2022-03-13T05:30:00Z	PT30M
519	519	368	418	812	194	812	101	23	59	-94	0	2022-03-13T06:00:00Z	PT30M
651	651	475	551	879	255	879	100	24	52	-94	0	2022-03-13T06:30:00Z	PT30M
772	772	570	659	918	279	918	112	26	44	-94	0	2022-03-13T07:00:00Z	PT30M
878	878	649	764	947	296	947	113	27	37	-95	0	2022-03-13T07:30:00Z	PT30M
967	967	724	843	963	313	963	123	28	29	-96	0	2022-03-13T08:00:00Z	PT30M
1038	1038	747	911	982	261	982	126	28	22	-97	0	2022-03-13T08:30:00Z	PT30M
1088	1088	761	956	989	226	989	132	29	15	-101	0	2022-03-13T09:00:00Z	PT30M
1116	1116	748	973	979	172	979	143	29	7	-112	0	2022-03-13T09:30:00Z	PT30M

APPENDIX F3: API FORECAST 14TH MARCH 2022

Ghi	Ghi90	Ghi10	Ebh	Dni	Dni10	Dni90	Dhi	air_temp	Zenith	Azimuth	cloud_op	period_end	Period
1123	1123	731	977	978	145	978	146	30	3	166	0	2022-03-13T10:00:00Z	PT30M
1108	1108	704	967	979	132	979	140	30	9	108	0	2022-03-13T10:30:00Z	PT30M
1072	1072	681	939	972	134	972	133	32	16	100	0	2022-03-13T11:00:00Z	PT30M
1005	1015	629	864	939	118	957	140	32	23	97	0	2022-03-13T11:30:00Z	PT30M
898	939	551	729	851	90	935	168	32	31	95	4	2022-03-13T12:00:00Z	PT30M
795	844	446	615	781	52	908	179	30	38	95	5	2022-03-13T12:30:00Z	PT30M
673	735	351	488	704	34	872	184	30	46	94	8	2022-03-13T13:00:00Z	PT30M
553	611	264	371	617	21	821	181	29	53	94	9	2022-03-13T13:30:00Z	PT30M
421	478	189	256	529	15	753	164	28	61	93	11	2022-03-13T14:00:00Z	PT30M
299	339	129	159	425	12	655	139	28	68	93	11	2022-03-13T14:30:00Z	PT30M
172	200	71	74	307	8	504	98	27	76	93	13	2022-03-13T15:00:00Z	PT30M
59	74	23	11	65	6	171	48	25	83	93	21	2022-03-13T15:30:00Z	PT30M
0	0	0	0	0	0	0	0	23	91	93	36	2022-03-13T16:00:00Z	PT30M
0	0	0	0	0	0	0	0	21	98	93	42	2022-03-13T16:30:00Z	PT30M
0	0	0	0	0	0	0	0	19	106	94	40	2022-03-13T17:00:00Z	PT30M
0	0	0	0	0	0	0	0	19	113	94	40	2022-03-13T17:30:00Z	PT30M
0	0	0	0	0	0	0	0	18	121	94	39	2022-03-13T18:00:00Z	PT30M
0	0	0	0	0	0	0	0	17	128	95	39	2022-03-13T18:30:00Z	PT30M
0	0	0	0	0	0	0	0	17	136	95	39	2022-03-13T19:00:00Z	PT30M
0	0	0	0	0	0	0	0	17	143	96	39	2022-03-13T19:30:00Z	PT30M
0	0	0	0	0	0	0	0	17	150	98	40	2022-03-13T20:00:00Z	PT30M
0	0	0	0	0	0	0	0	17	158	101	34	2022-03-13T20:30:00Z	PT30M
0	0	0	0	0	0	0	0	16	165	106	24	2022-03-13T21:00:00Z	PT30M
0	0	0	0	0	0	0	0	16	172	121	13	2022-03-13T21:30:00Z	PT30M
0	0	0	0	0	0	0	0	16	176	-170	4	2022-03-13T22:00:00Z	PT30M
0	0	0	0	0	0	0	0	16	171	-116	0	2022-03-13T22:30:00Z	PT30M
0	0	0	0	0	0	0	0	16	164	-104	0	2022-03-13T23:00:00Z	PT30M
0	0	0	0	0	0	0	0	16	156	-100	0	2022-03-13T23:30:00Z	PT30M
0	0	0	0	0	0	0	0	14	149	-98	0	3/14/2022	PT30M
0	0	0	0	0	0	0	0	14	142	-96	0	2022-03-14T00:30:00Z	PT30M
0	0	0	0	0	0	0	0	14	134	-95	0	2022-03-14T01:00:00Z	PT30M
0	0	0	0	0	0	0	0	14	127	-95	0	2022-03-14T01:30:00Z	PT30M
0	0	0	0	0	0	0	0	14	119	-94	0	2022-03-14T02:00:00Z	PT30M
0	0	0	0	0	0	0	0	14	112	-94	0	2022-03-14T02:30:00Z	PT30M
0	0	0	0	0	0	0	0	14	104	-93	0	2022-03-14T03:00:00Z	PT30M
0	0	0	0	0	0	0	0	14	97	-93	0	2022-03-14T03:30:00Z	PT30M
4	4	2	1	6	0	6	4	14	89	-93	0	2022-03-14T04:00:00Z	PT30M
97	97	45	43	252	12	252	54	17	82	-93	0	2022-03-14T04:30:00Z	PT30M
228	228	104	138	501	18	501	90	19	74	-93	0	2022-03-14T05:00:00Z	PT30M
368	368	172	274	688	25	688	94	21	67	-93	0	2022-03-14T05:30:00Z	PT30M
507	507	244	397	773	28	773	110	23	59	-93	0	2022-03-14T06:00:00Z	PT30M
638	638	319	528	837	37	837	110	24	52	-93	0	2022-03-14T06:30:00Z	PT30M
758	758	416	633	878	57	878	123	25	44	-94	0	2022-03-14T07:00:00Z	PT30M
862	862	499	737	908	79	908	124	26	37	-94	0	2022-03-14T07:30:00Z	PT30M
946	950	566	803	918	90	927	142	27	29	-95	0	2022-03-14T08:00:00Z	PT30M
1009	1018	596	854	921	83	944	154	28	22	-96	0	2022-03-14T08:30:00Z	PT30M
1038	1069	589	844	870	59	945	193	28	14	-99	2	2022-03-14T09:00:00Z	PT30M
1042	1093	576	808	814	45	940	233	29	7	-109	4	2022-03-14T09:30:00Z	PT30M
1028	1098	567	760	760	40	926	268	29	2	162	6	2022-03-14T10:00:00Z	PT30M
1001	1079	547	726	735	37	907	274	30	9	106	7	2022-03-14T10:30:00Z	PT30M

APPENDIX F4: API FORECAST 15TH MARCH 2022

Ghi	Ghi90	Ghi10	Ebh	Dni	Dni10	Dni90	Dhi	air_temp	Zenith	Azimuth	cloud_op	period_end	Period
938	1040	516	634	659	35	882	303	30	16	99	9	2022-03-14T11:00:00Z	PT30M
869	980	483	554	602	34	852	315	30	23	96	11	2022-03-14T11:30:00Z	PT30M
770	900	410	438	511	24	814	331	29	31	95	14	2022-03-14T12:00:00Z	PT30M
654	808	331	305	387	15	782	349	28	38	94	18	2022-03-14T12:30:00Z	PT30M
528	697	234	189	272	8	737	338	28	46	93	24	2022-03-14T13:00:00Z	PT30M
402	577	151	100	165	3	680	302	26	53	93	30	2022-03-14T13:30:00Z	PT30M
297	444	98	59	123	2	601	237	25	61	93	33	2022-03-14T14:00:00Z	PT30M
190	308	57	25	68	3	492	165	24	68	93	38	2022-03-14T14:30:00Z	PT30M
99	175	24	8	36	0	336	90	23	76	93	43	2022-03-14T15:00:00Z	PT30M
28	58	5	1	6	0	78	27	21	83	93	54	2022-03-14T15:30:00Z	PT30M
0	0	0	0	0	0	0	0	19	91	93	68	2022-03-14T16:00:00Z	PT30M
0	0	0	0	0	0	0	0	19	98	93	73	2022-03-14T16:30:00Z	PT30M
0	0	0	0	0	0	0	0	19	106	93	72	2022-03-14T17:00:00Z	PT30M
0	0	0	0	0	0	0	0	19	113	94	71	2022-03-14T17:30:00Z	PT30M
0	0	0	0	0	0	0	0	19	121	94	72	2022-03-14T18:00:00Z	PT30M
0	0	0	0	0	0	0	0	19	128	94	71	2022-03-14T18:30:00Z	PT30M
0	0	0	0	0	0	0	0	18	136	95	70	2022-03-14T19:00:00Z	PT30M
0	0	0	0	0	0	0	0	17	143	96	68	2022-03-14T19:30:00Z	PT30M
0	0	0	0	0	0	0	0	17	151	97	65	2022-03-14T20:00:00Z	PT30M
0	0	0	0	0	0	0	0	17	158	100	63	2022-03-14T20:30:00Z	PT30M
0	0	0	0	0	0	0	0	16	165	104	62	2022-03-14T21:00:00Z	PT30M
0	0	0	0	0	0	0	0	16	172	118	66	2022-03-14T21:30:00Z	PT30M
0	0	0	0	0	0	0	0	16	176	-168	77	2022-03-14T22:00:00Z	PT30M
0	0	0	0	0	0	0	0	16	171	-114	77	2022-03-14T22:30:00Z	PT30M
0	0	0	0	0	0	0	0	17	164	-103	73	2022-03-14T23:00:00Z	PT30M
0	0	0	0	0	0	0	0	17	156	-99	56	2022-03-14T23:30:00Z	PT30M
0	0	0	0	0	0	0	0	16	149	-97	22	3/15/2022	PT30M
0	0	0	0	0	0	0	0	16	142	-95	0	2022-03-15T00:30:00Z	PT30M
0	0	0	0	0	0	0	0	16	134	-95	0	2022-03-15T01:00:00Z	PT30M
0	0	0	0	0	0	0	0	14	127	-94	0	2022-03-15T01:30:00Z	PT30M
0	0	0	0	0	0	0	0	14	119	-94	0	2022-03-15T02:00:00Z	PT30M
0	0	0	0	0	0	0	0	14	112	-93	0	2022-03-15T02:30:00Z	PT30M
0	0	0	0	0	0	0	0	14	104	-93	0	2022-03-15T03:00:00Z	PT30M
0	0	0	0	0	0	0	0	16	97	-93	0	2022-03-15T03:30:00Z	PT30M
4	4	1	1	6	0	6	4	18	89	-93	0	2022-03-15T04:00:00Z	PT30M
101	101	27	49	288	0	288	52	19	82	-93	0	2022-03-15T04:30:00Z	PT30M
232	232	68	147	533	4	533	86	21	74	-93	0	2022-03-15T05:00:00Z	PT30M
372	372	114	280	711	4	711	92	23	67	-93	0	2022-03-15T05:30:00Z	PT30M
510	510	172	400	779	8	779	109	25	59	-93	0	2022-03-15T06:00:00Z	PT30M
641	641	244	533	853	11	853	108	26	52	-93	0	2022-03-15T06:30:00Z	PT30M
761	761	335	639	889	21	889	120	27	44	-93	0	2022-03-15T07:00:00Z	PT30M
865	865	407	742	926	28	926	122	27	37	-94	0	2022-03-15T07:30:00Z	PT30M
952	952	486	816	934	41	934	136	28	29	-94	0	2022-03-15T08:00:00Z	PT30M
1024	1024	520	885	956	41	956	138	28	22	-95	0	2022-03-15T08:30:00Z	PT30M
1073	1073	541	924	951	38	951	148	29	14	-98	0	2022-03-15T09:00:00Z	PT30M
1091	1102	539	921	928	33	953	168	29	7	-106	1	2022-03-15T09:30:00Z	PT30M
1065	1108	521	844	845	26	950	220	29	2	157	4	2022-03-15T10:00:00Z	PT30M
1016	1093	503	759	768	25	954	257	29	9	103	7	2022-03-15T10:30:00Z	PT30M
968	1059	487	697	726	26	952	270	29	16	97	8	2022-03-15T11:00:00Z	PT30M
896	1002	471	608	661	29	937	288	30	23	95	10	2022-03-15T11:30:00Z	PT30M

APPENDIX F5: API FORECAST 16TH MARCH 2022

Ghi	Ghi90	Ghi10	Ebh	Dni	Dni10	Dni90	Dhi	air_temp	Zenith	Azimuth	cloud_op	period_end	Period
810	927	417	520	607	24	933	289	30	31	94	12	2022-03-15T12:00:00Z	PT30M
700	833	345	391	496	16	902	309	28	38	93	15	2022-03-15T12:30:00Z	PT30M
573	724	250	261	375	9	874	312	28	46	93	20	2022-03-15T13:00:00Z	PT30M
446	603	163	151	251	3	818	294	26	53	93	25	2022-03-15T13:30:00Z	PT30M
331	472	108	90	185	2	763	241	25	61	93	29	2022-03-15T14:00:00Z	PT30M
223	335	65	43	116	3	646	179	24	68	92	33	2022-03-15T14:30:00Z	PT30M
125	198	31	18	76	0	525	106	22	76	92	36	2022-03-15T15:00:00Z	PT30M
42	74	9	3	21	0	164	38	21	83	93	42	2022-03-15T15:30:00Z	PT30M
0	0	0	0	0	0	0	0	21	91	93	49	2022-03-15T16:00:00Z	PT30M
0	0	0	0	0	0	0	0	19	98	93	55	2022-03-15T16:30:00Z	PT30M
0	0	0	0	0	0	0	0	19	106	93	61	2022-03-15T17:00:00Z	PT30M
0	0	0	0	0	0	0	0	19	113	93	66	2022-03-15T17:30:00Z	PT30M
0	0	0	0	0	0	0	0	18	121	93	72	2022-03-15T18:00:00Z	PT30M
0	0	0	0	0	0	0	0	18	128	94	73	2022-03-15T18:30:00Z	PT30M
0	0	0	0	0	0	0	0	18	136	94	72	2022-03-15T19:00:00Z	PT30M
0	0	0	0	0	0	0	0	18	143	95	70	2022-03-15T19:30:00Z	PT30M
0	0	0	0	0	0	0	0	17	151	96	69	2022-03-15T20:00:00Z	PT30M
0	0	0	0	0	0	0	0	17	158	99	66	2022-03-15T20:30:00Z	PT30M
0	0	0	0	0	0	0	0	17	165	103	65	2022-03-15T21:00:00Z	PT30M
0	0	0	0	0	0	0	0	17	173	116	64	2022-03-15T21:30:00Z	PT30M
0	0	0	0	0	0	0	0	17	177	-166	65	2022-03-15T22:00:00Z	PT30M
0	0	0	0	0	0	0	0	17	171	-111	67	2022-03-15T22:30:00Z	PT30M
0	0	0	0	0	0	0	0	16	164	-102	68	2022-03-15T23:00:00Z	PT30M
0	0	0	0	0	0	0	0	16	156	-98	69	2022-03-15T23:30:00Z	PT30M
0	0	0	0	0	0	0	0	16	149	-96	70	3/16/2022	PT30M
0	0	0	0	0	0	0	0	16	141	-95	70	2022-03-16T00:30:00Z	PT30M
0	0	0	0	0	0	0	0	16	134	-94	69	2022-03-16T01:00:00Z	PT30M
0	0	0	0	0	0	0	0	14	127	-94	68	2022-03-16T01:30:00Z	PT30M
0	0	0	0	0	0	0	0	14	119	-93	67	2022-03-16T02:00:00Z	PT30M
0	0	0	0	0	0	0	0	14	112	-93	66	2022-03-16T02:30:00Z	PT30M
0	0	0	0	0	0	0	0	14	104	-93	65	2022-03-16T03:00:00Z	PT30M
0	0	0	0	0	0	0	0	16	97	-92	64	2022-03-16T03:30:00Z	PT30M
2	6	0	0	0	0	12	2	17	89	-92	61	2022-03-16T04:00:00Z	PT30M
41	100	4	1	8	0	276	39	19	82	-92	58	2022-03-16T04:30:00Z	PT30M
101	231	12	4	16	0	519	96	19	74	-92	56	2022-03-16T05:00:00Z	PT30M
176	368	27	10	28	0	701	165	22	67	-92	52	2022-03-16T05:30:00Z	PT30M
262	504	53	20	40	0	761	241	23	59	-92	48	2022-03-16T06:00:00Z	PT30M
361	635	89	41	67	0	844	319	24	52	-92	43	2022-03-16T06:30:00Z	PT30M
470	753	139	78	108	1	869	392	25	44	-93	37	2022-03-16T07:00:00Z	PT30M
578	856	201	135	170	3	912	442	26	37	-93	32	2022-03-16T07:30:00Z	PT30M
666	945	245	185	212	3	918	480	27	29	-93	29	2022-03-16T08:00:00Z	PT30M
735	1015	278	232	251	3	937	502	28	22	-94	27	2022-03-16T08:30:00Z	PT30M
777	1064	287	247	256	3	935	529	28	14	-96	27	2022-03-16T09:00:00Z	PT30M
816	1093	301	283	285	3	940	533	28	7	-103	25	2022-03-16T09:30:00Z	PT30M
832	1100	316	300	300	3	936	531	28	2	150	24	2022-03-16T10:00:00Z	PT30M
853	1085	334	368	373	4	941	484	28	9	100	21	2022-03-16T10:30:00Z	PT30M
842	1051	348	398	414	6	937	444	28	16	96	19	2022-03-16T11:00:00Z	PT30M
827	994	369	445	483	11	924	382	28	23	94	16	2022-03-16T11:30:00Z	PT30M
775	920	342	438	512	10	921	336	28	31	93	15	2022-03-16T12:00:00Z	PT30M
671	827	278	329	417	7	887	342	27	38	93	18	2022-03-16T12:30:00Z	PT30M

APPENDIX F6: API FORECAST 17TH MARCH 2022

Ghi	Ghi90	Ghi10	Ebh	Dni	Dni10	Dni90	Dhi	air_temp	Zenith	Azimuth	cloud_op	period_end	Period
518	720	180	165	238	3	867	353	26	46	92	27	2022-03-16T13:00:00Z	PT30M
375	598	105	65	109	2	804	309	25	53	92	37	2022-03-16T13:30:00Z	PT30M
251	467	53	24	50	0	757	226	25	61	92	46	2022-03-16T14:00:00Z	PT30M
154	330	26	9	24	0	626	145	24	68	92	53	2022-03-16T14:30:00Z	PT30M
76	195	9	2	10	0	504	73	23	76	92	60	2022-03-16T15:00:00Z	PT30M
25	72	2	1	6	0	153	24	22	83	92	64	2022-03-16T15:30:00Z	PT30M
0	0	0	0	0	0	0	0	21	91	92	65	2022-03-16T16:00:00Z	PT30M
0	0	0	0	0	0	0	0	19	98	92	66	2022-03-16T16:30:00Z	PT30M
0	0	0	0	0	0	0	0	19	106	92	67	2022-03-16T17:00:00Z	PT30M
0	0	0	0	0	0	0	0	18	113	93	69	2022-03-16T17:30:00Z	PT30M
0	0	0	0	0	0	0	0	17	121	93	70	2022-03-16T18:00:00Z	PT30M
0	0	0	0	0	0	0	0	17	128	93	70	2022-03-16T18:30:00Z	PT30M
0	0	0	0	0	0	0	0	17	136	94	70	2022-03-16T19:00:00Z	PT30M
0	0	0	0	0	0	0	0	17	143	95	70	2022-03-16T19:30:00Z	PT30M
0	0	0	0	0	0	0	0	17	151	96	71	2022-03-16T20:00:00Z	PT30M
0	0	0	0	0	0	0	0	17	158	98	71	2022-03-16T20:30:00Z	PT30M
0	0	0	0	0	0	0	0	17	166	101	72	2022-03-16T21:00:00Z	PT30M
0	0	0	0	0	0	0	0	17	173	113	73	2022-03-16T21:30:00Z	PT30M
0	0	0	0	0	0	0	0	17	177	-163	74	2022-03-16T22:00:00Z	PT30M
0	0	0	0	0	0	0	0	17	171	-109	76	2022-03-16T22:30:00Z	PT30M
0	0	0	0	0	0	0	0	16	164	-100	77	2022-03-16T23:00:00Z	PT30M
0	0	0	0	0	0	0	0	16	156	-97	78	2022-03-16T23:30:00Z	PT30M
0	0	0	0	0	0	0	0	16	149	-95	79	3/17/2022	PT30M
0	0	0	0	0	0	0	0	16	141	-94	79	2022-03-17T00:30:00Z	PT30M
0	0	0	0	0	0	0	0	16	134	-94	77	2022-03-17T01:00:00Z	PT30M
0	0	0	0	0	0	0	0	16	126	-93	75	2022-03-17T01:30:00Z	PT30M
0	0	0	0	0	0	0	0	16	119	-93	73	2022-03-17T02:00:00Z	PT30M
0	0	0	0	0	0	0	0	14	111	-92	71	2022-03-17T02:30:00Z	PT30M
0	0	0	0	0	0	0	0	14	104	-92	68	2022-03-17T03:00:00Z	PT30M
0	0	0	0	0	0	0	0	16	97	-92	64	2022-03-17T03:30:00Z	PT30M
2	6	0	0	0	0	12	2	17	89	-92	60	2022-03-17T04:00:00Z	PT30M
44	100	3	1	11	0	276	42	18	82	-92	55	2022-03-17T04:30:00Z	PT30M
111	228	9	6	23	0	507	105	19	74	-92	51	2022-03-17T05:00:00Z	PT30M
204	366	25	20	51	0	694	184	21	67	-92	44	2022-03-17T05:30:00Z	PT30M
310	502	50	45	87	0	751	264	22	59	-92	38	2022-03-17T06:00:00Z	PT30M
434	630	90	105	171	0	836	328	23	52	-92	31	2022-03-17T06:30:00Z	PT30M
571	748	156	212	295	1	856	358	24	44	-92	23	2022-03-17T07:00:00Z	PT30M
706	852	229	368	462	4	900	337	25	37	-92	17	2022-03-17T07:30:00Z	PT30M
825	939	299	517	591	6	905	308	26	29	-93	12	2022-03-17T08:00:00Z	PT30M
927	1008	363	661	714	9	924	264	27	22	-93	8	2022-03-17T08:30:00Z	PT30M
1015	1057	380	794	817	8	921	220	28	14	-95	4	2022-03-17T09:00:00Z	PT30M
1052	1085	400	838	844	9	923	214	28	7	-100	3	2022-03-17T09:30:00Z	PT30M
1027	1092	372	760	760	7	918	267	28	1	140	5	2022-03-17T10:00:00Z	PT30M
992	1077	351	704	713	6	925	287	27	9	98	7	2022-03-17T10:30:00Z	PT30M
923	1042	323	596	620	5	920	327	27	16	94	11	2022-03-17T11:00:00Z	PT30M
861	987	306	529	575	5	908	331	27	23	93	12	2022-03-17T11:30:00Z	PT30M
770	914	261	431	502	4	908	338	27	31	92	15	2022-03-17T12:00:00Z	PT30M
650	821	202	290	367	3	872	360	26	38	92	20	2022-03-17T12:30:00Z	PT30M
519	714	140	169	243	1	856	350	25	46	92	27	2022-03-17T13:00:00Z	PT30M
383	593	83	74	123	0	789	308	24	53	92	35	2022-03-17T13:30:00Z	PT30M

APPENDIX F7: API FORECAST 17TH MARCH 2022

Ghi	Ghi90	Ghi10	Ebh	Dni	Dni10	Dni90	Dhi	air_temp	Zenith	Azimuth	cloud_op	period_end	Period
271	463	51	36	74	0	744	235	24	61	92	41	2022-03-17T14:00:00Z	PT30M
172	328	26	14	38	0	614	157	23	68	92	47	2022-03-17T14:30:00Z	PT30M
90	192	12	5	21	0	483	85	22	76	92	52	2022-03-17T15:00:00Z	PT30M
31	71	4	1	6	0	147	30	22	83	92	56	2022-03-17T15:30:00Z	PT30M
0	0	0	0	0	0	0	0	21	91	92	57	2022-03-17T16:00:00Z	PT30M
0	0	0	0	0	0	0	0	19	98	92	58	2022-03-17T16:30:00Z	PT30M
0	0	0	0	0	0	0	0	19	106	92	60	2022-03-17T17:00:00Z	PT30M
0	0	0	0	0	0	0	0	18	113	92	62	2022-03-17T17:30:00Z	PT30M
0	0	0	0	0	0	0	0	18	121	92	63	2022-03-17T18:00:00Z	PT30M
0	0	0	0	0	0	0	0	17	128	93	65	2022-03-17T18:30:00Z	PT30M
0	0	0	0	0	0	0	0	17	136	93	66	2022-03-17T19:00:00Z	PT30M
0	0	0	0	0	0	0	0	17	143	94	67	2022-03-17T19:30:00Z	PT30M
0	0	0	0	0	0	0	0	17	151	95	68	2022-03-17T20:00:00Z	PT30M
0	0	0	0	0	0	0	0	17	158	97	69	2022-03-17T20:30:00Z	PT30M
0	0	0	0	0	0	0	0	16	166	100	70	2022-03-17T21:00:00Z	PT30M
0	0	0	0	0	0	0	0	16	173	110	65	2022-03-17T21:30:00Z	PT30M
0	0	0	0	0	0	0	0	16	177	-159	57	2022-03-17T22:00:00Z	PT30M
0	0	0	0	0	0	0	0	16	171	-106	46	2022-03-17T22:30:00Z	PT30M
0	0	0	0	0	0	0	0	16	164	-99	34	2022-03-17T23:00:00Z	PT30M
0	0	0	0	0	0	0	0	16	156	-96	21	2022-03-17T23:30:00Z	PT30M
0	0	0	0	0	0	0	0	16	149	-94	8	3/18/2022	PT30M
0	0	0	0	0	0	0	0	16	141	-94	0	2022-03-18T00:30:00Z	PT30M
0	0	0	0	0	0	0	0	16	134	-93	0	2022-03-18T01:00:00Z	PT30M
0	0	0	0	0	0	0	0	14	126	-93	0	2022-03-18T01:30:00Z	PT30M
0	0	0	0	0	0	0	0	14	119	-92	0	2022-03-18T02:00:00Z	PT30M
0	0	0	0	0	0	0	0	14	111	-92	0	2022-03-18T02:30:00Z	PT30M
0	0	0	0	0	0	0	0	14	104	-92	0	2022-03-18T03:00:00Z	PT30M
0	0	0	0	0	0	0	0	16	96	-92	0	2022-03-18T03:30:00Z	PT30M
7	7	2	2	12	0	12	4	17	89	-92	0	2022-03-18T04:00:00Z	PT30M
102	102	22	39	228	0	228	63	18	81	-91	0	2022-03-18T04:30:00Z	PT30M
231	231	51	145	526	4	526	87	19	74	-91	0	2022-03-18T05:00:00Z	PT30M
368	368	89	257	633	2	633	110	21	66	-91	0	2022-03-18T05:30:00Z	PT30M
504	504	126	392	761	2	761	113	22	59	-91	0	2022-03-18T06:00:00Z	PT30M
633	633	178	505	804	3	804	128	23	51	-91	0	2022-03-18T06:30:00Z	PT30M
753	753	247	625	869	7	869	128	24	44	-91	0	2022-03-18T07:00:00Z	PT30M
856	856	316	715	883	9	883	141	25	36	-92	0	2022-03-18T07:30:00Z	PT30M

APPENDIX G: PUBLICATIONS

The following papers have been published from this thesis

[1] Apiyo E. O, Muriithi C. M. & Ngoo L. M. (2022), “Impact of Energy Management in a Solar PV Microgrid”. *International Journal of Engineering and Advanced Technology (IJEAT)*, 11(5), 65-73.

[2] Apiyo E. O, Muriithi C. M. & Ngoo L. M. (2021), “Modelling and Energy Management Strategy in a Grid Connected Solar PV-battery Energy Storage System”. *Journal of Agriculture Science & Technology (JAGST)*, 20 (3), 4-15.